Science of the Total Environment 575 (2017) 545–563

Contents lists available at ScienceDirect

Science of the Total Environment

journal homepage: www.elsevier.com/locate/scitotenv

Seasonal exports and drivers of dissolved inorganic and organic carbon, carbon dioxide, methane and $\delta^{13}C$ signatures in a subtropical river network

Marnie L. Atkins [a,b,*], Isaac R. Santos [a,b], Damien T. Maher [a,b]

[a] School of Environment, Science and Engineering, Southern Cross University, Lismore, NSW 2480, Australia
[b] National Marine Science Centre, Southern Cross University, Coffs Harbour, NSW 2450, Australia

HIGHLIGHTS

- Seasonal measurements of carbon were undertaken in 28 sites in 3 subcatchments.
- Seasonal rates of DIC and DOC exports, and CO_2 and CH_4 evasion were calculated.
- Hydrology controlled carbon export and CO_2 evasion was the main carbon export pathway.
- Riverine carbon dynamics may be influenced by climate change.

GRAPHICAL ABSTRACT

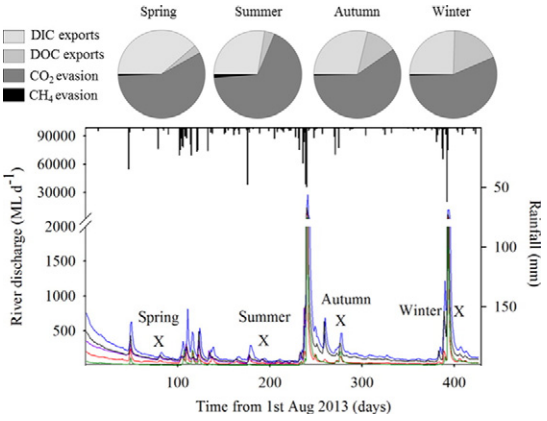

ARTICLE INFO

Article history:
Received 30 May 2016
Received in revised form 1 September 2016
Accepted 2 September 2016
Available online 28 September 2016

Editor: D. Barcelo

Keywords:
Aquatic carbon
Radon
Keeling plots
Climate change
Greenhouse gases
Carbon budget

ABSTRACT

Riverine systems act as important aquatic conduits for carbon transportation between atmospheric, terrestrial and oceanic pools, yet the magnitude of these exports remain poorly constrained. Interconnected creek and river sites (n = 28) were sampled on a quarterly basis in three subcatchments of the subtropical Richmond River Catchment (Australia) to investigate spatial and temporal dynamics of dissolved inorganic carbon (DIC), dissolved organic carbon (DOC), carbon dioxide (CO_2), methane (CH_4), and carbon stable isotope ratios ($\delta^{13}C$). The study site is an area of high interest due to potential unconventional gas (coal seam gas or coal bed methane) development. DIC exports were driven by groundwater discharge with a small contribution by in situ DOC remineralization. The DIC exports showed seasonal differences ranging from 0.10 to 0.27 mmol m^{-2} catchment d^{-1} (annual average 0.17 mmol m^{-2} catchment d^{-1}) and peaked during winter when surface water discharge was highest. DOC exports (sourced from terrestrial organic matter) had an annual average 0.07 mmol m^{-2} catchment d^{-1} and were 1 to 2 orders of magnitude higher during winter compared to spring and summer. CO_2 evasion rates (annual average of 347 mmol m^{-2} water area d^{-1}) were ~2.5 fold higher during winter compared to spring. Methane was always supersaturated (0.19 to 62.13 μM), resulting from groundwater discharge and stream-bed methanogenesis. Methane evasion was highly variable across the seasons with an annual average of 3.05 mmol m^{-2} water area d^{-1}. During drier conditions, stable isotopes implied enhanced CH_4 oxidation.

* Corresponding author at: School of Environment, Science and Engineering, Southern Cross University, Lismore, NSW 2480, Australia
E-mail address: marnieatkins1@gmail.com (M.L. Atkins).

http://dx.doi.org/10.1016/j.scitotenv.2016.09.020
0048-9697/

Overall, carbon losses from the catchment were dominated by CO_2 evasion (60%) followed by DIC exports (30%), DOC exports (9%) and CH_4 evasion (<1%). Our results demonstrated broad catchment scale spatial and temporal variability in carbon dynamics, and that groundwater discharge and rain events controlled carbon exports.

1. Introduction

Understanding carbon transport, storage and transformation along the aquatic continuum has become increasingly important when considering the implications of climate change, and the subsequent effects on regional and global carbon budgets. Rivers are major conduits for carbon exchange between terrestrial, atmospheric and oceanic reservoirs (Huang et al., 2012; Palmer et al., 2001). Rivers evade an estimated 0.23 Pg C as atmospheric carbon dioxide (CO_2) and export 0.71 Pg C to the coastal ocean (Cole et al., 2007). Recent efforts in constraining the role of rivers in the global C cycle have been significant. However, large uncertainties exist due to the lack of seasonal measurements at the catchment scale, and the lack of integrated measurements of how the major carbon species (i.e., dissolved inorganic carbon (DIC), dissolved organic carbon (DOC), CO_2 and methane (CH_4)) interact and contribute to carbon budgets.

Riverine dissolved carbon (DIC and DOC) can display high temporal and spatial variability, and is controlled by a number of factors such as climatic conditions, hydrological cycles, source characteristics, and both terrestrial and in situ processes. Identifying dissolved carbon sources can help characterise possible changes brought about by climate change. Riverine DIC sources include carbonate dissolution, silicate weathering, aquatic respiration, atmospheric CO_2 invasion and soil respiration derived CO_2 transported via groundwater or overland flow (Atkins et al., 2013; Santos et al., 2015). Processes that remove DIC from rivers include CO_2 evasion to the atmosphere, aquatic photosynthesis and carbonate mineral precipitation (Atekwana and Krishnamurthy, 1998; Kanduc et al., 2007). Riverine DOC is derived from in situ production, atmospheric deposition and terrestrial organic matter sources (Avery et al., 2003; Benner and Opsahl, 2001; Onstad et al., 2000). DOC is depleted within rivers via photo-degradation, flocculation and microbial consumption (Amon and Benner, 1996; Sholkovitz, 1976). While there are studies that focus on the control of DOC quantity in headwater systems (Hope et al., 1994; Turmel et al., 2005), studies that investigate comparisons between tributary creeks and adjoining large river systems lag behind in the literature.

Methane dynamics have been well documented in estuarine and marine environments (Borges and Abril, 2011; Call et al., 2015; Middelburg et al., 2002; Santos et al., 2009), and freshwater lentic systems such as lakes and reservoirs (DelSontro et al., 2010; Schubert et al., 2010). However, less is known about riverine CH_4 dynamics. Fresh water environments are generally supersaturated in CH_4 due to delivery of CH_4 rich groundwater to surface waters, along with the anaerobic degradation of organic matter in sediments (Crawford and Stanley, 2015; Stanley et al., 2015). Methane oxidation and CH_4 evasion rates are key factors controlling CH_4 concentrations in surface waters (Jones and Mulholland, 1998a). Annual CH_4 evasion from fluvial environments is estimated to be 26.8 Tg CH_4 which is comparable to both lakes and wetlands (Stanley et al., 2015). However, the temporal and spatial coverage of data used for this recent estimate is limited and, as such, the estimate of global CH_4 flux from rivers is highly uncertain.

Hydrology plays a major role in the transport and transformation of riverine carbon. Large rainfall events can export significant quantities of carbon from headwater streams to downstream estuaries (Huntington and Aiken, 2013; Westhorpe and Mitrovic, 2012). During rainfall events, DOC is generally flushed from soils into adjacent surface waters where it is transformed in situ or delivered to the coastal ocean (Griffiths et al., 2012; Moyer et al., 2015; Mulholland, 2003). Further, increased surface water turbulence enhances the gas transfer velocity (Ho et al., 2016; Raymond et al., 2012), leading to greater gaseous carbon evasion. Drier periods often increase water residence times and allow for in situ processes to take effect and transform aquatic carbon (Mann et al., 2014). During dry periods, evaporation effects are more influential which can increase carbon species concentrations. Groundwater discharge can increase following precipitation events due to a higher water table (Peterson et al., 2010) but it can also dominate during dry periods when many riverine systems are only supported by groundwater input (Hrachowitz et al., 2011; Mann et al., 2014). Characterising groundwater dynamics can be complex and often groundwater dynamics within riverine systems remains poorly understood. Much less is known about the relationship between carbon transport and groundwater discharge in rivers. However, groundwater discharge can be influential in delivering carbon to surface waters during both dry and wet conditions (Atkins et al., 2013; Sadat-Noori et al., 2015).

Using carbon stable isotope ratios ($\delta^{13}C$) has enabled (1) characterisation of the carbon origin, (2) insight into the various in situ carbon transformations and (3) quantification of inputs from natural or anthropogenic processes (Atekwana and Krishnamurthy, 1998; Barth et al., 2003; Schulte et al., 2011). Thus stable isotope techniques complement large spatial and long temporal investigations by providing information on processes shaping observed patterns in carbon (Maher et al., 2015; Schulte et al., 2011). Generally, riverine $\delta^{13}C$-DIC is depleted by addition of biogenic CO_2 derived from respiration (Taylor and Fox, 1996; Yang et al., 1996) while $\delta^{13}C$-DIC enrichment results from photosynthetic processes preferentially removing ^{12}C (Flintrop et al., 1996; Pawellek and Veizer, 1994). Biogenic sources deplete the CH_4 signature while CH_4 oxidation preferentially oxidises $^{12}CH_4$, creating an enriched $\delta^{13}C$-CH_4 signal (Whiticar and Faber, 1986; Whiticar et al., 1986).

In this riverine study, carbon exports and evasion, and stable isotope ratios for DIC, DOC, CO_2 and CH_4 were measured from four seasonal sampling campaigns over one year in three subcatchments from the Richmond River Catchment (Australia). This paper builds on the river carbon literature by (1) simultaneously quantifying the four major dissolved carbon species and their stable isotope signature, (2) focusing on a relatively less studied subtropical region, and (3) assessing whether groundwater is a major driver of carbon dynamics in rivers. The study site is an area of high interest for methane and hydrology investigations because the flagged development of coal seam gas fields in the area may modify current conditions (Iverach et al., 2015; Tan et al., 2015). In the Condamine River, Australia (within a large CSG field), studies concluded that extensive methane seepage at several locations within the river is associated with coal seam CH_4 (Apte et al., 2014). Considering that no baseline research was undertaken in the Condamine River prior to CSG development, the study could not determine if gas migration pathways were a natural phenomenon or influenced by CSG extraction methods. This case reflects the importance of understanding riverine carbon cycling prior to fossil fuel mining.

2. Methods

2.1. Study site

Surface water samples were collected from the Richmond River Catchment (Fig. 1), a sub-tropical catchment (~7000 km^2) located in the far north coast of New South Wales (NSW), Australia (DPI, 2012). The Richmond River is ~170 km in length and passes several townships

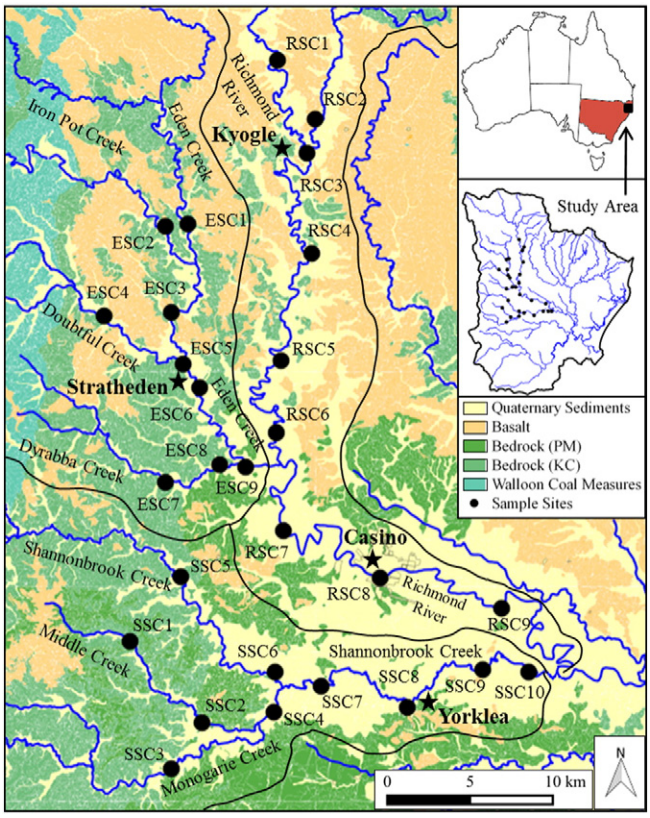

Fig. 1. Map of the Richmond River Catchment. The three subcatchments are outlined by the black lines. RSC sites are the Richmond Subcatchment, ESC sites are the Eden Subcatchment and SSC sites are the Shannonbrook Subcatchment. All subcatchments drain a larger area than shown on the main map (see catchment inset). Bedrock PM is the Piora Member and bedrock KC is the Kangaroo Creek Sandstone Member. Four gauging stations are shown (Kyogle, Stratheden, Casino and Yorklea) while the Wiangaree gauging station is located north of Kyogle on the Richmond River. The same river samples were used in a companion paper describing radon and ion observations (Atkins et al., 2016a).

before meeting the Pacific Ocean at Ballina. The upland ranges bordering the catchment reach elevations over 1000 m and remain mostly forested while the lower coastal floodplains are used for agricultural activities and residential purposes. A mild sub-tropical climate delivers high annual rainfall to the inland areas (1200 mm) and along the coastal fringe (1800 mm), with the wet, warmer months (December to March) typically receiving ~65% of the total annual precipitation (Atkins et al., 2013 and references therein). Although annual rainfall is high, the entire region can experience long drought periods associated with El Niño–Southern Oscillation (ENSO) cycles. Averaged river discharge between 2003 and 2013 recorded at the Casino gauging station was 1367 ± 270 ML d^{-1}. During the study, the averaged river discharge was 369.6 ML d^{-1} (Table 1), demonstrating the year was much drier than the previous 10 years.

The study area extended from north of Kyogle to south of Casino, over ~70 km and was divided into 3 sub catchments based on underlying geological characteristics and surface water chemistry (Fig. 1; Table 1). The Eden Subcatchment (ESC) is a small subcatchment (718 km^2) with interconnected creeks, draining mostly basaltic rocks and soils (Atkins et al., 2015). The Shannonbrook Subcatchment (SSC) is located in the lower catchment, south of Casino, and also represents a small interconnected creek system (606 km^2). The underlying geology is mainly sandstone bedrock with basaltic hills to the west (Drury, 1982). The Eden Subcatchment drains into the Richmond Subcatchment (the largest subcatchment with an area of 1220 km^2) which includes the Richmond River, extending from north of Kyogle to south of Casino. The upper subcatchment area was characterised by steep incised embankments and underlying basaltic rocks while the lower subcatchment (past Casino) sloped gently with wider river stretches and underlying sandstone bedrock.

The bedrock and basalts in the subcatchments are underlain by the Walloon Coal Measures which contain considerable coal seam gas (CSG) reserves. Approximately 50 CSG exploration wells have been drilled (with no associated infrastructure). Mining operations were suspended in March 2013 but the region remains a potential CSG development area. A number of studies have investigated carbon and groundwater dynamics in the lower catchment including the estuary and fringing wetlands (Atkins et al., 2013; de Weys et al., 2011; Gatland et al., 2014; Ruiz-Halpern et al., 2015), but no carbon data are available on the mid/upper catchment sections investigated here. This study is part of a series of baseline studies in the Richmond River Catchment (a region where coal seam gas extraction may occur) and builds on previous groundwater (Atkins et al., 2015, 2016b), surface water (Atkins et al., 2016a) and atmospheric baseline investigations (Maher et al., 2014; Tait et al., 2015).

2.2. Sampling

A total of 28 creek and river sites were sampled quarterly during one year to capture seasonal and hydrological variations in carbon dynamics. Field investigations were performed during spring (16th–17th October 2013), summer (11th–12th February 2014), autumn (7th – 8th May 2014) and winter (2nd and 3rd September 2014, technically spring but titled winter for convenience and due to low water temperatures). These river samples used for carbon analysis were also used in a recent study where radon and major ions provided insight into groundwater-surface water connectivity (Atkins et al., 2016a). River discharge data (ML d^{-1}) and rainfall data (mm) were obtained from five gauging stations on the Richmond River (n = 3), Eden Creek (n = 1) and Shannonbrook Creek (n = 1) (Office of Water, 2015) (Fig. 2). Bridge access allowed sampling from the surface water centre while creek bank

Table 1
Comparison table for the three subcatchments (Richmond, Eden and Shannonbrook). Groundwater observations were from Atkins et al. (2015). Note groundwater endmembers were identical for the Richmond Subcatchment and the Eden Subcatchment.

	Richmond Subcatchment	Eden Subcatchment	Shannonbrook Subcatchment
System	River	Creek	Creek
Length of surface water (km)	111	50.3	81.8
Underlying geology	Predominantly basalt	Basalt	Sandstone bedrock
Land area (km^2)	1220	718	606
Surface water discharge (ML d^{-1})	379.8	103.9	55.4
Groundwater endmembers			
DIC (mM)	7.15 ± 0.75	7.15 ± 0.75	7.59 ± 0.85
δ^{13}C-DIC (‰)	−11.18 ± 0.90	−11.18 ± 0.90	−14.47 ± 0.98
CH_4 (μM)	6.39 ± 2.85	6.39 ± 2.85	28.07 ± 22.81
δ^{13}C-CH_4 (‰)	−59.07 ± 3.49	−59.07 ± 3.49	−59.87 ± 7.60

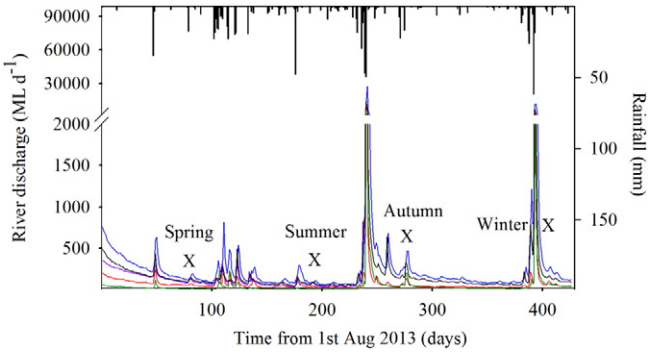

Fig. 2. Precipitation and river discharge over the annual period. Sampling campaigns are indicated by X. River discharge is shown from five gauging stations. The purple line is the Wiangaree station, the black line is the Kyogle station, the red line is the Stratheden station, the blue line is the Casino station and the green line is the Yorklea station. Note the higher precipitation and river discharge before the autumn and winter sampling events.

edge access allowed sampling 1 m or more from the bank edge. River water samples were taken at a depth of ~50 cm. Surface water velocity was measured by timing a piece of floating debris travelling 2 m and taking the average of three repeats. Wind data was obtained from meteorological stations in Casino and Lismore (BOM, 2014). Surface water velocity and wind data were used to determine the gas transfer velocity (k) at each site (which was required to calculate gas evasion, see below). The creek slope was determined using a digital elevation model and GIS. Groundwater samples were taken in a previous study (Atkins et al., 2015).

A calibrated handheld YSI-85 water quality multiprobe was used on site to measure pH, dissolved oxygen (DO), temperature and specific conductivity. The pH was calibrated using 4.00 and 7.00 standards [National Bureau of Standards (NBS) scale]. For specific conductivity, calibrations were completed with a 1413 μS cm^{-1} standard and deionised water, to cover the observed range of surface water conductivities. Discrete samples were collected for DIC, DOC, CO_2, CH_4, carbon stable isotopes and radon (^{222}Rn). Samples for DIC, DOC, δ^{13}C-DIC and δ^{13}C-DOC were collected with a sample rinsed 60 mL polypropylene syringe and filtered through 0.7 mm Whatman GF/F filters, leaving no headspace or bubbles. Samples were injected into acid rinsed and precombusted (at 450 °C for 4 h) 40 mL VOC borosilicate vials containing a preservation solution of 100 μL of saturated $HgCl_2$. Duplicate samples for CO_2, CH_4, δ^{13}C-CO_2 and δ^{13}C-CH_4 were collected in pre-rinsed gas tight bottles (215 mL), and treated with saturated $HgCl_2$ solution (200 μL), before being sealed with a cap and septum without leaving a headspace. Radon samples were collected in airtight 6 L HDPE plastic bottles (Lee and Kim, 2006). All samples were kept on ice until stored in laboratory refrigerators or freezers as appropriate.

2.3. Analytical methods

For CO_2 and CH_4 concentration and isotope samples, a 50 mL zero air headspace (free of CO_2 and CH_4) was introduced into the bottle and samples were left overnight for equilibration. A 40 mL equilibrated gas sample was extracted from the bottle and injected into a Tedlar gas bag with 400 mL zero air and the sample was analysed by a Picarro G2201-I which measured CO_2 and CH_4 concentrations and stable carbon isotope ratios by cavity ring down spectroscopy (Crosson, 2008). Guaranteed precision by the manufacturer are 210 ppb + 0.05% of reading for CO_2 and 60 ppb + 0.05% of reading for CH_4. CO_2 and CH_4 concentrations were determined using Henry's Law and the stable carbon isotope ratios were recorded as per mil (‰), relative to V-PDB (Gatland et al., 2014). An OI Scientific Aurora 1030 TOC analyser coupled to a Thermo Fisher Delta V isotope ratio mass spectrometer (IRMS) was used to analyse DIC, DOC, δ^{13}C-DIC and δ^{13}C-DOC with analytical uncertainties better than 5% (Maher and Eyre, 2011). HCO_3^- concentrations were calculated using pH and DIC concentrations on the Excel macro CO_2 System (CO_2SYS) (Pelletier et al., 2007), using the NBS pH scale and the Dickson and Millero (1987) carbonate system constants. Radon samples were analysed using a RAD-7 (Durridge and Co) radon-in-air monitor modified for radon-in-water analysis (Burnett et al., 2001) by fitting a closed air loop connecting the sample bottle, RAD-7 and Drierite column (to maintain humidity below 10%). Rapid radon equilibration between the air and water (approximately 50 min) was achieved by recirculating the air through an air stone (submerged in the sample) via an internal pump in the RAD-7. Equations described by Lee and Kim (2006) were used to convert radon observations in the air stream to dissolved radon. Counting uncertainties of better than 5% were achieved by analysing samples for at least 2 h.

2.4. Calculations

Statistical differences were tested for each parameter on both a spatial and temporal basis. Normality was initially established using the Shapiro Wilk's W test. ANOVA tests were performed and when a significant difference was identified, a comparison of means test was applied. For normal distributions, t-tests (selecting equal or unequal variances with an f-test) were used and for non-parametric data, the Mann Whitney U test was used. When comparing a normal and non-normal dataset, the Mann Whitney U test was used. DIC and DOC exports were calculated by multiplying the surface water discharge by the DIC or DOC concentration from the final site in each subcatchment. This value was then divided by the total area of each subcatchment to give DIC and DOC exports in mmol m^{-2} catchment d^{-1}. To calculate the river discharge at the final site of each subcatchment (gauging stations were located upstream of the final site), we used the ratio of the catchment area upstream of the gauging stations and the total area of the catchment upstream of the point of interest. This approach assumes homogenous rainfall and runoff coefficients across the catchment. This ratio was then multiplied by the river discharge at the gauging site to calculate the river discharge at the final site in each subcatchment. Apparent oxygen utilisation (AOU) was calculated by the following equation:

$$AOU = [O_2*] - [O_2] \quad (1)$$

where [O_2*] is the oxygen concentration (μmol) at 100% saturation, calculated as a function of temperature and salinity (Benson and Krause, 1984), and [O_2] is the measured dissolved oxygen concentration (μmol). Excess CO_2 was defined as the CO_2 emitted to the atmosphere after complete water-air equilibration (Abril et al., 2000) and was calculated by the difference between in situ CO_2 concentration (i.e. $CO_{2(aq)} + H_2CO_{3(aq)}$) and CO_2 concentrations at atmospheric equilibrium (i.e. pCO_2 of 400 μatm).

The air-water CO_2 and CH_4 exchange rate was estimated from the gas transfer velocity (k), gas solubility and the gas concentration gradient between the air and water phase.

$$F = k\alpha(G_{water} - G_{air}) \quad (2)$$

Where F is the gas flux (mmol m^{-2} d^{-1}), k is the gas transfer velocity (m d^{-1}), α is the solubility co-efficient of the respective gas (ie. CO_2 or CH_4), G_{water} is the partial pressure of gas in water (μatm), and G_{air} is the partial pressure of gas in the atmosphere (μatm). Positive values indicate evasion to the atmosphere while negative values indicate a net gas invasion into the surface water. CO_2 and CH_4 solubility coefficients were determined according to Weiss (1974) and Yamamoto et al. (1976), respectively. The atmospheric partial pressure of CO_2 and CH_4 was assumed to be 400 and 1.8 μatm, respectively.

The largest source of uncertainty when calculating gas evasion rates is determining the k value. Environmental conditions within the study

Table 2
Seasonal precipitation values 14 days prior to sampling, wind speeds recorded for both sampling days and surface water discharge measured at five gauging stations. The Richmond Subcatchment had three gauging stations (Wiangaree, Kyogle and Casino) (Fig. 1), and both the Eden Subcatchment and Shannonbrook Subcatchment had one gauging station each (Stratheden and Yorklea, respectively). Temporal and spatial average discharge values are shown. Note SC = Subcatchment.

Season	Precipitation 14 days prior (mm)	Wind speeds Day 1 ($m\ s^{-1}$)	Wind speeds Day 2 ($m\ s^{-1}$)	Wiangaree gauging station ($ML\ d^{-1}$)	Kyogle gauging station ($ML\ d^{-1}$)	Casino gauging station ($ML\ d^{-1}$)	Stratheden gauging station ($ML\ d^{-1}$)	Yorklea gauging station ($ML\ d^{-1}$)	Average
Spring	3.0	1.39	0.28	78.4	90.4	117.0	44.5	4.3	64.1
Summer	12.5	1.67	1.67	41.8	58.8	87.3	25.2	0.8	43.0
Autumn	48.0	1.94	1.67	126.2	140.3	228.3	44.9	54.0	116.9
Winter	135.3	3.89	3.89	173.9	242.3	493.4	87.0	128.8	237.9

region need consideration when choosing an appropriate parametrization of k. Since k was not determined onsite at individual sites in this investigation, several different empirical relationships of k were used based on key factors for gas exchange in riverine environments such as slope, current velocity and wind speed. Therefore, four empirical functions (Borges et al., 2004; Raymond and Cole, 2001; Raymond et al., 2012 (2 equations were used from this paper)) for the gas transfer velocity were chosen which provided reasonable ranges of CO_2 and CH_4 evasion rates, and allowed comparisons to other investigations using similar empirical functions. For each site, gas evasion was calculated as the mean from the four empirical functions. From Raymond et al. (2012), two k_{600} parametrisations derived from 563 gas tracer experiments within streams were chosen where stream slope and velocity were incorporated:

$$k_{600} = 1162 \pm 192 \times S^{0.77\pm0.028} V^{0.85\pm0.045} \quad (3)$$

$$k_{600} = (VS)^{0.76\pm0.027} \times 951.5 \pm 144 \quad (4)$$

where k_{600} is the gas transfer velocity ($cm\ h^{-1}$) for a gas normalised to a Schmidt number of 600, V is stream current velocity ($m\ s^{-1}$) and S is stream slope (unitless). The wind driven parameterisation from Raymond and Cole (2001) acquired from several estuarine and riverine investigations was also used:

$$k_{600} = 1.91e^{0.35u} \quad (5)$$

where u is the wind speed measured at a height of 10 m ($m\ s^{-1}$) and averaged on the sampling day. Finally, the wind speed driven parameterisation of Borges et al. (2004) was used:

$$k_{600} = 5.141{u_{10}}^{0.758} \quad (6)$$

where u_{10} is the wind speed at a height of 10 m ($m\ s^{-1}$) and averaged on the sampling day.

3. Results

3.1. Hydrological characteristics

Precipitation and discharge varied among the four seasonal sampling periods in the three subcatchments (Fig. 2; Table 2). River discharge in spring and summer were much lower than both autumn and winter (Table 2). Averaged river discharge was highest in the Richmond Subcatchment due to its larger catchment area (Table 1). Average surface water temperatures reached 24.6 °C in the summer and approached 16 °C in autumn and winter while dissolved oxygen was highest in winter and lowest during autumn (Table 3). The pH values ranged seasonally by ~1 while specific conductivity was 2-fold higher in spring compared to winter (Table 3). During all seasons, the Shannonbrook Subcatchment had higher specific conductivity than the other subcatchments (Table 3).

3.2. DIC and DOC concentrations, exports and ratios

Both the DIC and DOC concentrations generally followed seasonal trends (Fig. 3a and b). DIC concentrations decreased 3-fold from spring through to winter while DOC concentrations followed an opposite trend, increasing 2-fold from spring through to winter (Table 3). DIC exports were highest during winter for the Richmond Subcatchment and during spring for the Eden Subcatchment while in the Shannonbrook Subcatchment, DIC exports were ~1 to 2 orders of magnitude higher in winter compared to spring and summer (Fig. 4; Table 4). DOC exports were ~1 order of magnitude higher during winter for the Richmond Subcatchment and the Eden Subcatchment, and ~2 orders of magnitude greater in winter for the Shannonbrook Subcatchment compared to spring and summer (Fig. 4; Table 4).

Antecedent precipitation and river discharge greatly influenced the DIC/DOC ratio, resulting in an exponential trend when plotted versus cumulative precipitation and cumulative river discharge over 2 weeks (Fig. 5). DIC exports dominated during spring in the Richmond Subcatchment (DIC/DOC = 13.38), Eden Subcatchment (12.06) and Shannonbrook Subcatchment (10.71). A clear decrease in DIC/DOC was found in the winter (1.21 to 1.65) (Fig. 4) due to an increase in DOC exports when discharge was higher. During spring and summer, DIC export was much higher than DOC export. While during autumn and winter, DOC and DIC export was similar.

DIC carbon stable isotopes followed a temporal (rather than spatial) trend with significantly depleted values in spring compared to winter (Fig. 6; Table 3). The DOC stable isotopes were also more depleted in spring compared to winter though there were no significant differences between winter and both summer and autumn. δ^{13}C-DOC values were significantly different in the Richmond Subcatchment compared to the other subcatchments (Table 3). The δ^{13}C-DIC in groundwater in the Richmond Subcatchment and the Eden Subcatchment was more enriched than the Shannonbrook Subcatchment (Atkins et al., 2015) (Table 1).

Keeling plots can identify the carbon source when a significant linear correlation exists between 1/concentration and δ^{13}C (using type 2 regression) (Keeling, 1958). During autumn, the Keeling plots indicated, the δ^{13}C-DIC source was -8.33 ± 0.54‰ and during winter the δ^{13}C-DIC source was -9.08 ± 0.56‰ (Fig. 7). The Richmond Subcatchment source was – 10.87 ± 0.53‰, the Eden Subcatchment was – 10.30 ± 0.41‰ and the Shannonbrook Subcatchment was – 9.03 ± 0.39‰. The Keeling plots suggested the DOC source during autumn had a δ^{13}C value of -18.72 ± 0.77‰ and during winter had a δ^{13}C value of -19.21 ± 0.77‰ (Fig. 7). The Keeling plots identified the DOC source for The Richmond Subcatchment (−21.00‰) was more depleted than DOC sources for both the Eden Subcatchment (−19.30‰) and the Shannonbrook Subcatchment (−19.38‰).

3.3. pCO_2 and CH_4

Surface water pCO_2 was ~600 to 5000% supersaturated in relation to the atmosphere (Fig. 3c). pCO_2 was both spatially and temporally variable (Table 3), and followed a decreasing seasonal trend from summer

Table 3
Seasonal (spring, summer, autumn and winter) and spatial (Richmond, Eden and Shannonbrook subcatchments) for surface water parameters. Uncertainties were calculated using rules of error propagation.

		Spring	Summer	Autumn	Winter	Richmond Subcatchment	Eden Subcatchment	Shannonbrook Subcatchment
Temp (°C)	Average	22.94	24.60	15.94	16.20	20.60	19.53	19.32
	Median	23.10	24.84	15.88	16.28	18.16	18.56	16.75
	St Error	1.28	1.32	0.82	0.84	1.29	1.20	1.16
Sp Cond (mS cm^{-1})	Average	0.65	0.62	0.49	0.36	0.31	0.51	0.75
	Median	0.44	0.41	0.41	0.29	0.31	0.42	0.69
	St Error	0.08	0.08	0.06	0.04	0.02	0.05	0.07
pH	Average	7.84	7.74	7.52	6.95	7.53	7.50	7.49
	Median	7.93	7.88	7.58	6.94	7.70	7.64	7.47
	St Error	0.40	0.39	0.38	0.35	0.39	0.39	0.37
DO (mg L^{-1})	Average	7.30	n/d	7.60	9.00	8.39	7.07	8.46
	Median	8.16	n/d	7.70	9.15	8.46	7.82	8.33
	St Error	0.54	n/d	0.43	0.48	0.44	0.50	0.65
DIC (mM)	Average	3.54	2.99	1.59 (a)	1.29 (a)	1.86 (b, d)	2.65 (b, c)	2.48 (c, d)
	Median	3.06	2.61	1.49	1.08	1.79	2.15	2.13
	St Error	0.32	0.29	0.16	0.14	0.18	0.33	0.24
δ^{13}C-DIC (‰)	Average	−9.03	−7.72	−5.45 (a)	−5.58 (a)	−6.83 (b, d)	−7.09 (b, c)	−6.83 (c, d)
	Median	−9.00	−7.55	−5.79	−5.38	−7.15	−7.49	−7.02
	St Error	0.48	0.40	0.48	0.37	0.49	0.49	0.47
DOC (mM)	Average	0.32 (a)	0.40	0.57 (a)	0.71	0.36	0.67 (b)	0.48 (b)
	Median	0.28	0.36	0.45	0.64	0.32	0.54	0.47
	St Error	0.03	0.04	0.07	0.07	0.03	0.08	0.03
δ^{13}C-DOC (‰)	Average	−26.40	−24.13 (a)	−23.24 (b)	−23.38 (a, b)	−25.10	−23.86 (c)	−23.86 (c)
	Median	−26.68	−24.51	−23.58	−23.20	−25.17	−24.36	−23.62
	St Error	1.34	1.14	1.20	1.21	1.28	1.25	1.20
pCO_2 (μatm)	Average	6197 (a, b)	7085 (a)	5247 (b)	4381	5617 (c)	6398 (c)	5163
	Median	5680	5840	5092	4241	5559	5806	4268
	St Error	387	705	247	247	184	351	546
CH_4 (μM)	Average	1.92 (a, b, c)	5.67 (a)	1.14 (b, d)	1.09 (c, d)	0.72	1.48	4.84
	Median	1.28	1.55	0.89	0.71	0.61	1.06	1.64
	St Error	0.53	2.44	0.15	0.19	0.07	0.27	1.68
δ^{13}C-CH_4 (‰)	Average	−49.06 (a)	−47.25 (a)	−53.02	−55.34	−51.70 (b, d)	−50.07 (b, c)	−52.11 (c, d)
	Median	−49.70	−47.18	−54.23	−57.12	−51.41	−50.60	−52.42
	St Error	0.76	0.96	1.20	1.17	1.05	1.16	0.98
Radon (Bq m^{-3})	Average	97.1 (a, b, c)	115.5 (a)	66.0 (b, d)	56.3 (c, d)	51.4 (e)	113.5	84.9 (e)
	Median	56.1	90.6	50.2	46.0	50.2	85.9	49.6
	St Error	28.3	25.8	15.7	14.5	12.5	23.6	21.6

Seasons or subcatchments with the same lowercase letter represent homogenous subsets (Mann Whitney *U* test or *t*-tests).
Tests were performed for DIC, δ^{13}C-DIC, DOC, δ^{13}C-DOC, pCO_2, CH_4, δ^{13}C-CH_4 and radon.

(7085 ± 705 μatm) through to winter (4381 ± 247 μatm) (Fig. 3c; Table 3). The Shannonbrook Subcatchment (5163 ± 546 μatm) was significantly different than both the Eden (6398 ± 351 μatm) and the Richmond (5617 ± 184 μatm) Subcatchment (Table 3). Excess CO_2 significantly correlated with apparent oxygen utilisation (AOU) for spring, autumn and winter (no oxygen data in summer), and within all subcatchments (Fig. 8). Methane ranged between 0.19 and 62.13 μM and decreased from summer (5.67 ± 2.44 μM) through to winter (1.09 ± 0.19 μM) (Fig. 3d; Table 3).

Average *k* values for each gas transfer velocity equation were 2.13 ± 0.22 m d^{-1} (Eq. (3)), 2.03 ± 0.19 m d^{-1} (Eq. (4)), 1.00 ± 0.04 m d^{-1} (Eq. (5)) and 2.03 ± 0.07 m d^{-1} (Eq. (6)). Average gas transfer velocities used to calculate CO_2 and CH_4 evasion rates were 1.21 ± 0.09 m d^{-1} for spring, 1.33 ± 0.07 m d^{-1} for summer, 1.50 ± 0.09 m d^{-1} for autumn and 3.09 ± 0.23 m d^{-1} for winter. Gas transfer velocities were higher in winter due to higher wind speeds (Table 2). Evasion rates were calculated on a creek and catchment basis for comparisons with both the literature, and with the DIC and DOC exports reported in this paper.

Carbon dioxide evasion followed a seasonal trend, significantly increasing from spring (234 ± 15 mmol m^{-2} water area d^{-1}) through to winter (564 ± 60 mmol m^{-2} water area d^{-1}) (Table 4). Carbon dioxide evasion was significantly higher in the Eden Subcatchment compared to both the Richmond and the Shannonbrook subcatchments. Methane evasion in all subcatchments followed similar trends with lower values during spring and autumn and significantly higher values during summer and winter (Table 4). Overall, atmospheric CH_4 evasion in the Shannonbrook Subcatchment was twice as high as the Eden Subcatchment and 5 times greater than the riverine Richmond Subcatchment (Table 4). δ^{13}C-CH_4 was more enriched in spring (−49.06 ± 0.76‰) and summer (−47.25 ± 0.96‰) and significantly more depleted during autumn (−53.02 ± 1.20‰) and winter (−55.34 ± 1.17‰) (Fig. 6; Table 3). δ^{13}C-CH_4 was not statistically different between the subcatchments.

Radon (a natural groundwater tracer) concentrations during summer (115.5 ± 25.8 Bq m^{-3}) were significantly different to both autumn (66.0 ± 15.7 Bq m^{-3}) and winter (56.3 ± 14.5 Bq m^{-3}) (Table 3; data originally reported in Atkins et al. (2016a)). Radon was significantly correlated to DIC in The Eden Subcatchment during spring ($r^2 = 0.52$, $p = 0.03$) and summer ($r^2 = 0.78$, $p < 0.01$) implying groundwater played a role in delivering DIC to surface waters. Overall, radon and pCO_2 ($r^2 = 0.29$, $p < 0.01$) and CH_4 ($r^2 = 0.16$, $p < 0.01$, $n = 109$) were significantly correlated (Fig. 9). Radon and CH_4 were significantly correlated for each individual season (except winter) and for each individual subcatchment (Fig. 9a and b). Radon and CH_4 were the most variable constituents measured during the study. Temporally, the coefficient of variation (CV) for radon was 135, 89, 74, and 91% (spring, summer, autumn and winter, respectively) and for CH_4 was 148, 228, 69, and 95%, respectively. Spatially, the CV for radon was 65, 93 and 122% (Richmond, Eden and Shannonbrook subcatchments, respectively) and for CH_4 was 61, 105 and 219%, respectively.

4. Discussion

Assessing carbon sources and drivers within riverine systems remains important to understand regional and global carbon budgets. When investigating creek tributaries and river stems, it is not unusual to find significant spatial (Khadka et al., 2014) and temporal (Cai et al.,

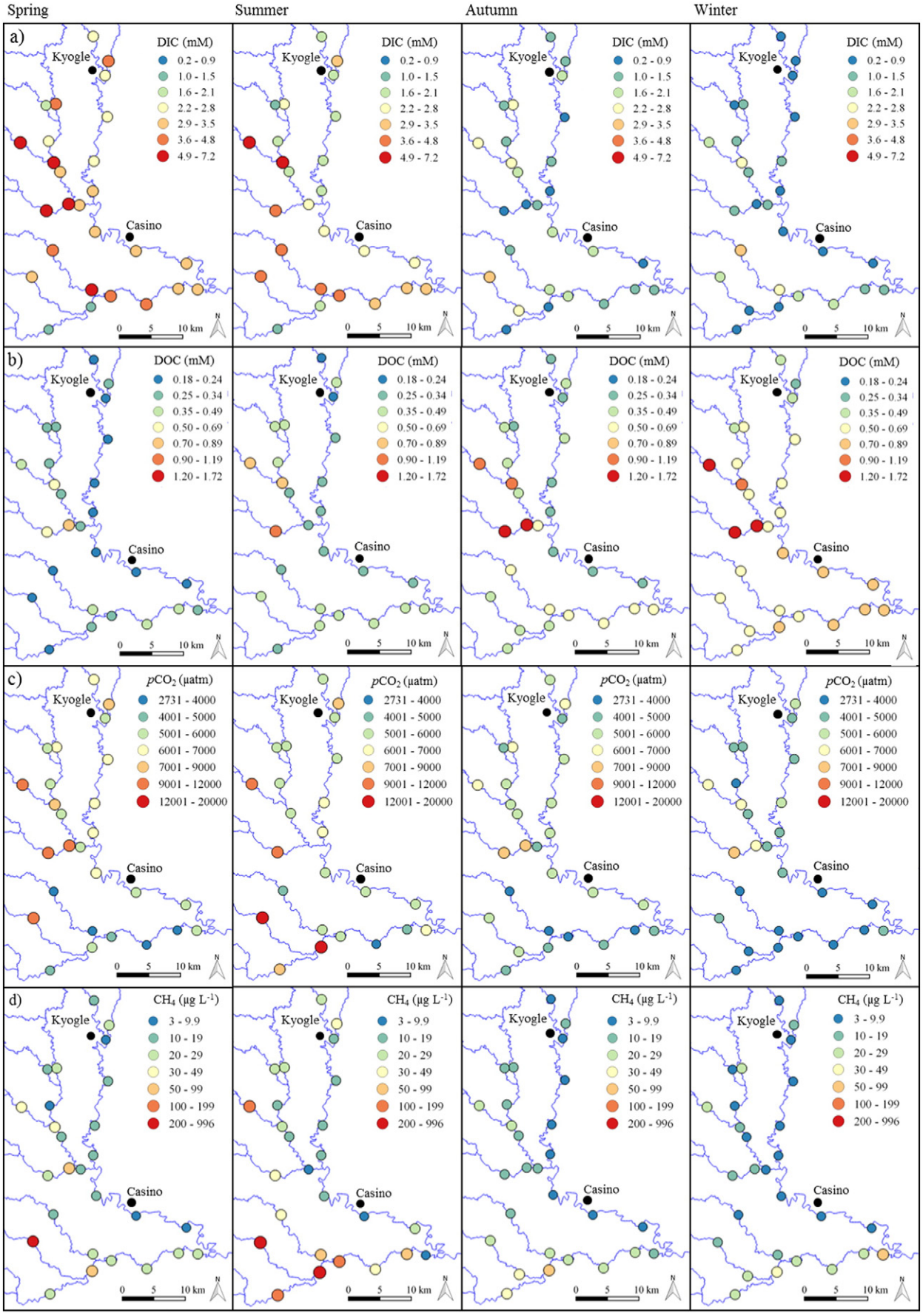

Fig. 3. a) DIC concentrations, b) DOC concentrations, c) pCO_2 values and d) CH_4 concentrations for each season (spring, summer, autumn and winter). Note DIC concentrations decreased through the seasons while DOC concentrations increased. For pCO_2 values and CH_4 concentrations, note the overall variability and decreased values from spring through to winter.

2008) variability due to the complex nature of catchment scale carbon dynamics. While the four sampling events (spring, summer, autumn and winter) may not represent the entire seasonal variability, contrasting seasonal and hydrological conditions were captured. To better understand seasonal carbon dynamics, higher temporal sampling resolution may be necessary.

4.1. Dissolved carbon exports and drivers

The spatial and temporal characterisation of dissolved carbon can provide insight into the major processes influencing dissolved carbon dynamics within riverine systems (Maher and Eyre, 2012; Mann et al., 2014; Striegl et al., 2007). In the Richmond River Catchment, DIC concentration and isotopes followed a temporal rather than spatial trend, and were controlled by hydrological variability in groundwater delivery and precipitation events. Aquatic photosynthesis during warmer months can decrease the DIC pool while simultaneously enriching δ^{13}C-DIC by preferentially removing the $^{12}CO_2$ isotopologue (Atekwana and Krishnamurthy, 1998). This process can reverse during cooler months when respiration becomes the dominant in situ process. However, in this investigation DIC was higher in the warmer months (depleted δ^{13}C-DIC) and lower in the cooler months (enriched δ^{13}C-DIC), suggesting that groundwater discharge overrode aquatic photosynthesis as the predominant control of the DIC pool during the drier seasons. In previous investigations in other rivers, lower rainfall periods increased evaporation within surface waters, often increasing the relative contribution of local and deep groundwater inputs over riverine DIC concentrations (Barth et al., 2003; Mann et al., 2014). These conditions were present during the drier spring and summer periods, resulting in high DIC concentrations coinciding with depleted δ^{13}C-DIC. The significant relationship between radon and DIC in the Eden Subcatchment, the overall higher radon concentrations during spring and summer, and the depleted groundwater δ^{13}C-DIC endmembers (Table 1), indicated that groundwater likely played a large role in delivering DIC to surface waters in the Richmond River Catchment during drier seasons. Coupling between DIC and groundwater have been found in previous riverine investigations (Atekwana and Krishnamurthy, 1998; Helie et al., 2002; Shin et al., 2011).

While respiration can be the major DIC source during cooler periods, hydrological conditions determined DIC exports in this study. Winter conditions produced the lowest DIC concentrations along with the highest DIC exports. High surface water discharge, not present in other seasons, was the main control on downstream DIC exports. In a spatial context, the Richmond Subcatchment had significantly lower DIC concentrations and depleted δ^{13}C-DIC than the other two subcatchments. However, the Richmond Subcatchment, with a surface water discharge over 3 times higher than the other two subcatchments, had the highest DIC export. Therefore DIC exports were driven by hydrology, as has been reported for a diversity of other catchments (e.g. Hossler and Bauer, 2013; Mann et al., 2014; Striegl et al., 2007).

Keeling plots showed that during autumn and winter, the δ^{13}C-DIC source was more depleted (Fig. 7), suggesting that during times of higher precipitation and river discharge, DIC was derived from a combination of groundwater and a more δ^{13}C depleted source (possibly in situ organic matter degradation). As DIC concentrations decreased, δ^{13}C-DIC values became more enriched, indicating aquatic photosynthesis and atmospheric CO_2 evasion exerted a control over the DIC pool (Aravena and Suzuki, 1990; Buhl et al., 1991; Flintrop et al., 1996; Yang et al., 1996) with both processes removing in-stream CO_2 (with a preferential removal of the $^{12}CO_2$ isotopologue), leading to a fractionation (enrichment) of the residual DIC. While the same processes for DIC transport and transformation were evident in other regions such as the Southern Han River (Shin et al., 2011) and the Rhone River system (Aucour et al., 1999), this may not always be the case. DIC in systems such as the Yukon River were controlled by respiration processes, with δ^{13}C-DIC more depleted as DIC concentrations increased (Striegl et al., 2007).

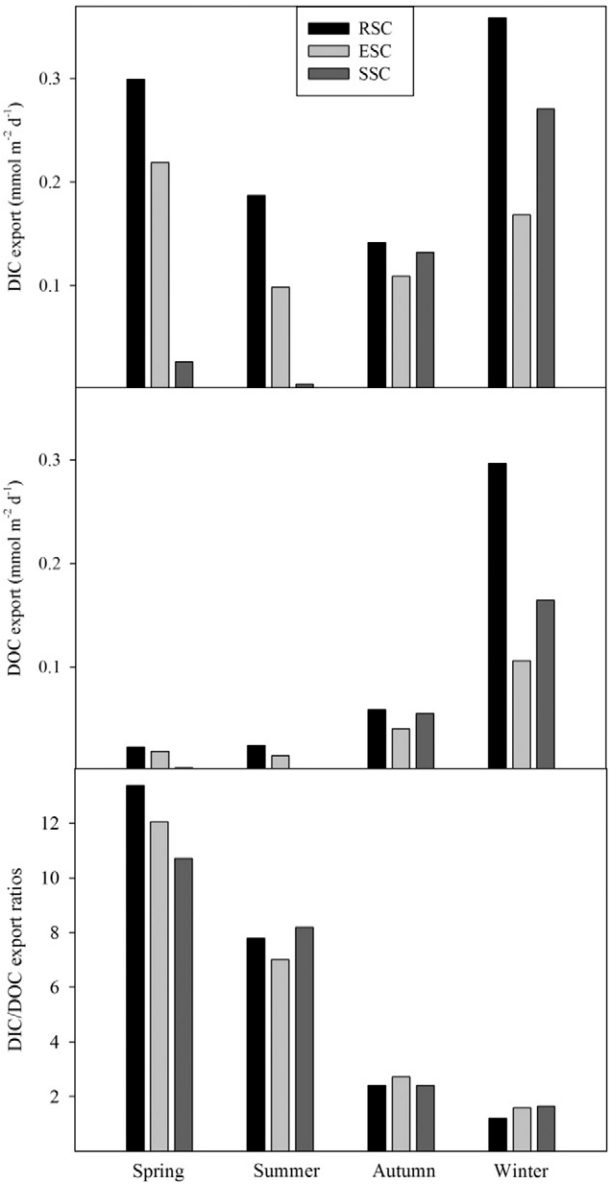

Fig. 4. DIC and DOC exports and ratios for the Richmond (RSC), Eden (ESC) and Shannonbrook (SSC) subcatchments during spring, summer, autumn and winter. The exports are calculated on a per catchment basis. Note the DIC/DOC ratios decreased seasonally due to the DIC and DOC exports being similar during winter.

The Keeling plots identified a dominant DIC source on a spatial basis that was marginally more enriched than the seasonal basis (in autumn and winter) (Fig. 7). The δ^{13}C-DIC values for both the Eden Subcatchment and the Richmond Subcatchment were similar to the groundwater endmember δ^{13}C-DIC values (-11.18 ± 0.90‰) (Table 1), indicating that DIC was likely derived from groundwater. However, the Shannonbrook Subcatchment groundwater δ^{13}C-DIC endmember was more depleted (-14.47 ± 0.98‰), indicating another DIC source or rapid isotopic enrichment of the DIC pool within surface waters. Despite differences in geology, topography and anthropogenic activities, all three subcatchments had signs that groundwater played an important (and in two subcatchments, a dominant) role in delivering DIC to the river.

One of the primary controls on riverine DOC exports are precipitation events delivering accumulated soil DOC to adjacent waters (Griffiths et al., 2012; Mulholland, 2003). This was observed during winter, when river discharge was highest, and DOC exports were

Table 4
Seasonal (spring, summer, autumn and winter) and spatial (Richmond, Eden and Shannonbrook subcatchments) for DIC and DOC exports, and CO_2 and CH_4 evasion.

		Spring	Summer	Autumn	Winter	Richmond Subcatchment	Eden Subcatchment	Shannonbrook Subcatchment
DIC export (mmol m^{-2} d^{-1}) catchment	Average	0.18	0.10	0.13	0.27	0.25	0.15	0.11
	Median	0.22	0.10	0.13	0.27	0.24	0.14	0.08
	St Error	0.08	0.05	0.01	0.05	0.05	0.03	0.06
DOC export (mmol m^{-2} d^{-1}) catchment	Average	0.01	0.01	0.05	0.19	0.10	0.04	0.06
	Median	0.02	0.01	0.05	0.16	0.04	0.03	0.03
	St Error	0.01	0.01	0.01	0.06	0.07	0.02	0.04
CO_2 evasion (mmol m^{-2} d^{-1}) water area	Average	234 (a)	278 (a, b)	311 (b)	564	310 (c)	457	299 (c)
	Median	187	224	286	408	297	326	310
	St Error	15	20	18	60	17	48	13
CH_4 evasion (mmol m^{-2} d^{-1}) water area	Average	1.68 (a)	5.56 (b)	1.76 (a)	3.32 (b)	1.04	2.61	5.36
	Median	1.01	2.04	1.13	2.03	0.86	1.52	2.83
	St Error	0.20	1.30	0.16	0.42	0.06	0.36	0.89

Seasons or subcatchments with the same lowercase letter represent homogenous subsets (Mann Whitney *U* test or *t*-tests).
Tests were performed for pCO_2 and CH_4 evasion.

more than one order of magnitude greater than the drier months. Flooding conditions flushed terrestrial DOC from upland areas into the river channel, and once in the river, to downstream locations. This has been showed in a diversity of both relatively undisturbed sites such as the Congo Basin (Mann et al., 2014), an Australian subtropical headwater stream (Looman et al., 2016) and Little River, Georgia (Mehring et al., 2013), and human influenced sites such as the Yellow River, China (Ran et al., 2013).

The Keeling plots showed the autumn and winter DOC source had a $\delta^{13}C$ value of $-18.72 \pm 0.77‰$ and $-19.21 \pm 0.77‰$, respectively (Fig. 7). This implied a terrestrial origin for DOC resulting from a combination of C3 and C4 plants ($-27‰$ and $-12‰$, respectively (Smith and Epstein, 1971)). C3 and C4 plants exist in the subcatchments which are dominated by a combination of forested areas and agricultural grasses. $\delta^{13}C$-DOC varied little within each subcatchment suggesting minimal biogeochemical processing during downstream riverine transit as found in previous studies (Striegl et al., 2007). During the drier seasons, $\delta^{13}C$-DOC was more depleted than autumn and winter, and the Keeling plots did not identify a dominant DOC source (Fig. 7), suggesting multiple processes controlled the DOC pool. River discharge was low and surface waters experienced a longer residence time which can lead to a shift from external sources (groundwater and surface runoff) to in situ sources (Hanley et al., 2013).

DOC concentrations and isotopes were significantly lower in the Richmond Subcatchment (river system) than both the Eden and Shannonbrook Subcatchments (creek systems) even though DOC exports were 2-fold higher. DOC transportation and in situ biological processing differs between creeks and rivers (Hanley et al., 2013). Due to longer residence times of large rivers compared to smaller creek headwaters, in situ aquatic processes (such as photodegradation, microbial remineralisation and sediments sorption) can exert a stronger control over the DOC pool in larger systems. Regardless of lower DOC concentrations and more depleted $\delta^{13}C$-DOC in the Richmond Subcatchment, the higher DOC exports reflect large discharge events control DOC aquatic transport as shown in other investigations (Dalzell et al., 2011; Griffiths et al., 2012; Mulholland, 2003).

DIC export was 3-fold greater than DOC export over the annual period (Fig. 10). Sadat-Noori et al. (2015) found a similar ratio of DIC:DOC exports, with DIC export contributing up to 70% of the dissolved carbon exports from an Australian subtropical estuary. Although overall DIC exports were much larger than DOC exports in the Richmond River Catchment, the relative importance of DIC and DOC exports varied seasonally. Antecedent precipitation and river discharge greatly influenced the DIC/DOC export ratio, resulting in an exponential trend when related to cumulative precipitation and cumulative river discharge over 2 weeks (Fig. 5). DOC exports rates approached DIC exports during times of increased precipitation. Overall annual DIC exports and DOC exports accounted 30% and 9% of the total carbon exports, respectively (Fig. 10).

4.2. Carbon dioxide evasion and drivers

The dominant processes controlling pCO_2 in river water are; (1) soil CO_2 respiration and subsequent CO_2 transportation through overland flow or groundwater input, (2) in situ organic matter decomposition and respiration, (3) atmospheric CO_2 evasion and (4) aquatic photosynthesis (Richey et al., 2002; Wang et al., 2007; Yao et al., 2007). The first two mechanisms increase pCO_2 while the latter two processes decrease pCO_2 (Li et al., 2012). Aqueous pCO_2 is also influenced by precipitation intensity and surface water discharge. During the drier seasons, slower flowing shallow surface water (<50 cm depth at some creek sites) created a concentrating effect, resulting in much higher pCO_2 than the wetter seasons (Fig. 3c). Increased rainfall during autumn and winter along with greater river discharge diluted CO_2 concentrations and enhanced CO_2 evasion to the atmosphere, resulting in lower pCO_2 values during these seasons. Overall, radon and pCO_2 were correlated ($r^2 = 0.29$, $p < 0.01$), implying groundwater inputs may have played a role in delivering CO_2 to surface waters (Atkins et al., 2013; Macklin et al., 2014; Perkins et al., 2015). Although groundwater inputs were likely delivering CO_2 to the system, it appeared that in situ biological processes and ecosystem respiration also exerted a strong control over surface water pCO_2 (Fig. 8).

Rivers are often supersaturated in pCO_2 because of high CO_2 inputs from groundwater and in situ respiration exceeding primary production. The net result is often high rates of CO_2 evasion to the atmosphere. Ubiquitous pCO_2 supersaturation in the Richmond River Catchment surface waters meant CO_2 evasion was always directed towards the atmosphere (Fig. 3c). While pCO_2 decreased with increasing river discharge, atmospheric CO_2 evasion followed an opposite trend due to higher transfer velocities with increased discharge in winter (Table 4). Therefore hydrology was the significant driver for CO_2 evasion as has been shown in other investigations (De Fátima et al., 2008; Maher et al., 2015; Ruiz-Halpern et al., 2015).

Globally, CO_2 evasion is thought to account for about 24% of carbon losses from rivers (Cole et al., 2007). Compared to other forms of carbon transport and transformation, CO_2 evasion was the most important carbon export pathway for each season and subcatchment (except for spring in the Richmond and Eden Subcatchment when DIC export was highest) (Fig. 10). CO_2 evasion accounted for 60% of the total catchment scale carbon export annually, and was on average the largest loss term from each of the subcatchments over the study (Fig. 10).

4.3. Methane evasion and drivers

Globally, river systems are often highly supersaturated in CH_4 with respect to the atmosphere (Borges et al., 2015; de Angelis and Lilley, 1987; Wallin et al., 2014). In the Richmond River Catchment, persistent CH_4 supersaturation (63 to 22,838 times greater than atmospheric

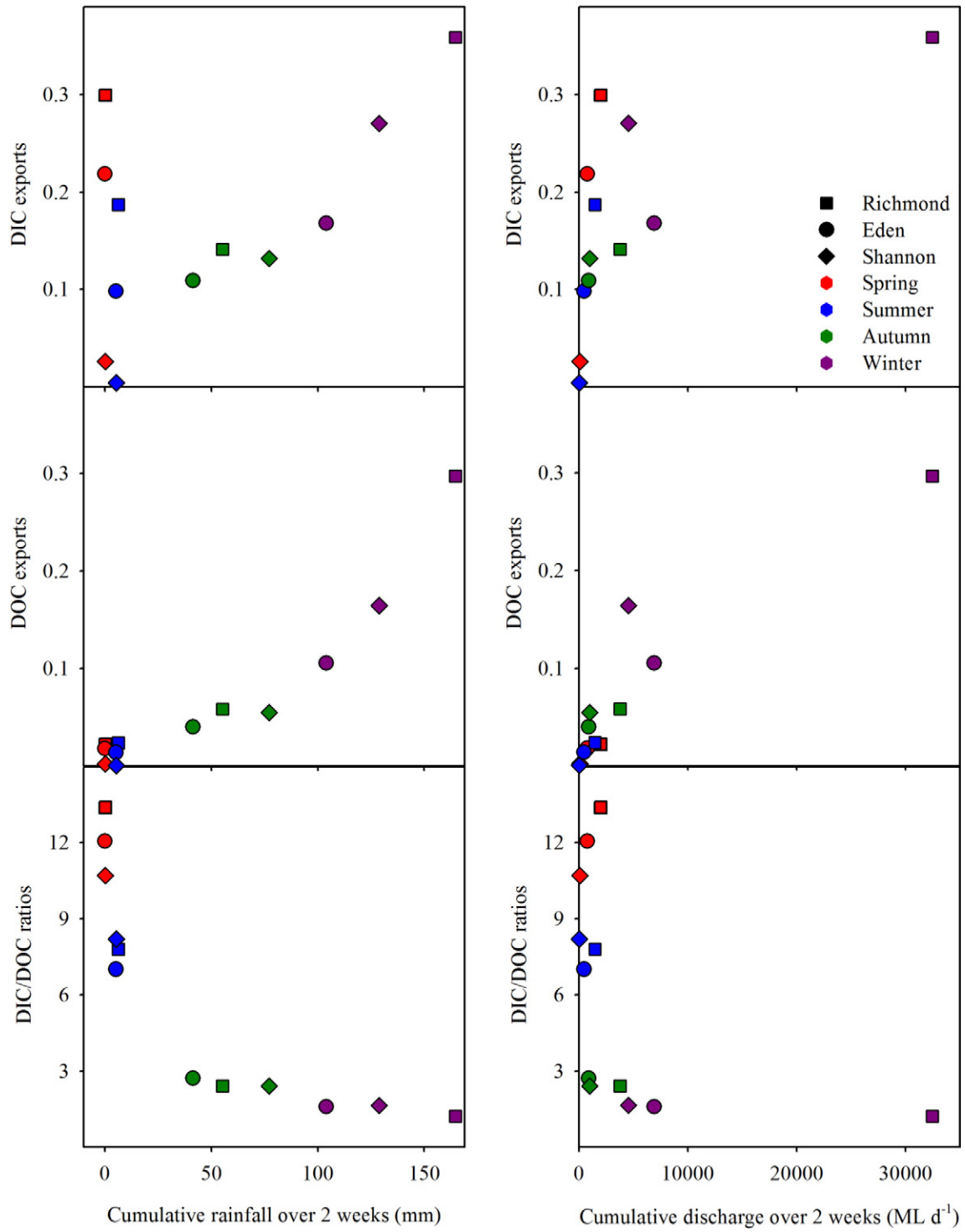

Fig. 5. DIC and DOC exports, and DIC/DOC ratios vs cumulative rainfall and cumulative water discharge over 2 weeks. The shapes represent the subcatchments (squares = Richmond, circles = Eden and diamonds = Shannonbrook) while the colour coding (hexagonal shapes) represents seasons (red = spring, blue = summer, green = autumn and purple = winter). Note the exponential trend for DIC/DOC ratios vs cumulative rainfall.

equilibrium) occurred in surface waters over the four seasons (Fig. 3d). Surface water methane is generally coupled to groundwater inputs (de Angelis and Lilley, 1987; Hope et al., 2001; Jones and Mulholland, 1998b; Santos et al., 2008) and in situ processes occurring in stream sediments (Heffernan et al., 2008; Wilcock and Sorrell, 2008). Radon correlated with CH_4 ($r^2 = 0.16$, $p < 0.01$, $n = 109$), implying some CH_4 was delivered to surface waters via groundwater inputs (Fig. 9). Methane concentrations were higher in the smaller subcatchments where the groundwater and in situ influence on surface water chemistry was likely greater than the larger riverine system (Table 3). During spring and summer, six sites existed either as disconnected pools or displayed extremely slow water flow, with three of these sites having the highest radon concentrations (430, 493, 617 Bq m^{-3}) and three sites showing the highest CH_4 levels (11.00, 25.54 and 62.13 μM) (Fig. 9a). The higher CH_4 and radon levels were likely associated in the higher sediment surface area to volume ratio in these pools, leading to

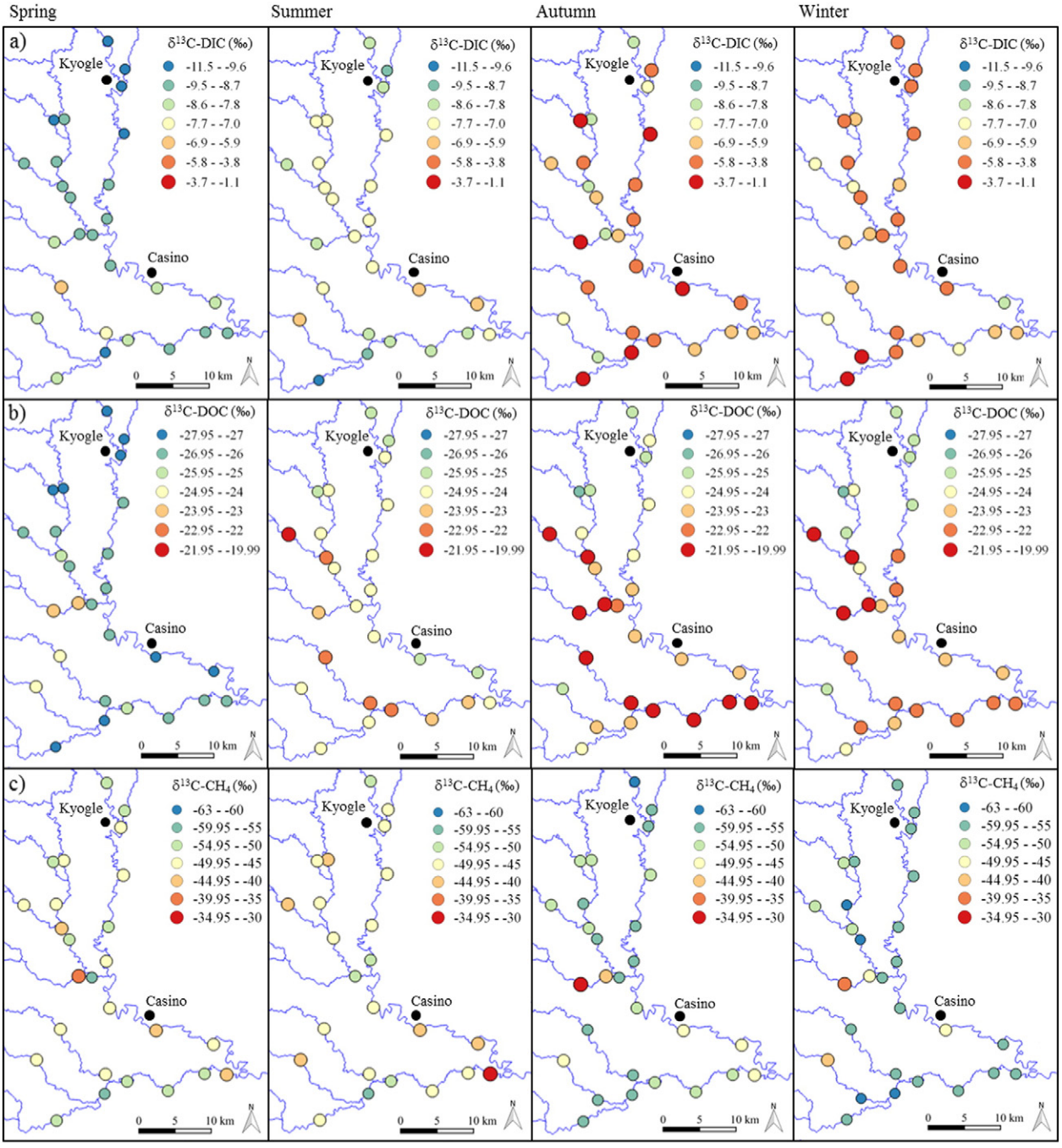

Fig. 6. a) δ^{13}C-DIC values, b) δ^{13}C-DOC and c) δ^{13}C-CH_4 for each season and subcatchment. Note the enrichment for both δ^{13}C-DIC and δ^{13}C-DOC through the seasons. δ^{13}C-CH_4 values became depleted from spring through to summer due to decreased CH_4 oxidation during both autumn and winter.

a concentrating effect. These environments were characterised by long residence times which allowed groundwater to continuously enter surface water with slow downstream dispersal.

Methane concentrations were ~5 times higher during summer compared to winter (Table 3). In river systems, warmer seasons appear to provide environments more favourable to methanogenesis (Campeau and Del Giorgio, 2014; Rulík et al., 2000) by creating anoxic conditions due to decreased dissolved oxygen solubility, by increased organic matter production (Garnier et al., 2013), and by increasing microbial production (Bergman et al., 2000; Whalen, 2005). During cooler periods, CH_4 production can decrease (Adrian et al., 1994) due to lower surface water temperatures, increased dissolved oxygen solubility and decreased microbial metabolism rates. Winter surface water temperatures were ~8 °C lower than summer, and winter DO levels were high at 9.0 mg L^{-1}, likely contributing to limited CH_4 production and/or increased CH_4 oxidation.

Greater river discharge during winter resulted in lower CH_4 concentrations yet increased CH_4 evasion (due to higher transfer velocities) which suggested hydrology was an important seasonal driver of CH_4 dynamics, as has been the case in other investigations (Abril et al., 2007; Kone et al., 2010; Middelburg et al., 2002). During wetter seasons, lower CH_4 concentrations may be attributed to limited in situ CH_4 production caused by disturbance (de Angelis and Scranton, 1993), greater atmospheric evasion rates (Anthony et al., 2012) and delivery of CH_4 poor surface water runoff causing river dilution (Hope et al., 2001). In the Richmond River Catchment during the drier seasons, the higher CH_4 concentrations (Fig. 3d) were likely attributed to groundwater discharge and in-stream anaerobic processes (Jones and Mulholland,

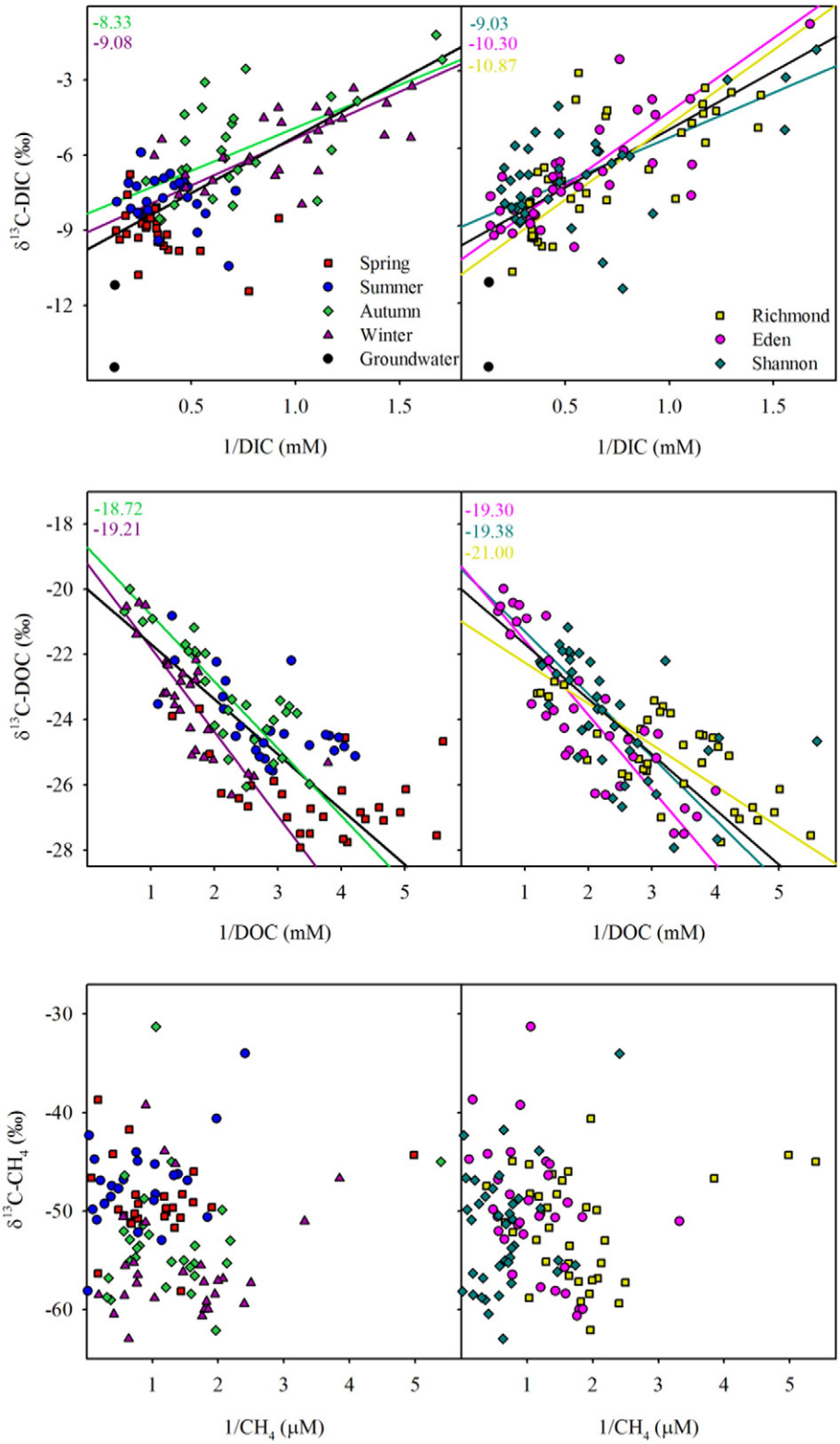

Fig. 7. Keeling plots of DIC, DOC and CH_4 for both seasons and subcatchments. Significant regressions are represented by the coloured lines and existed for DIC in autumn ($r^2 = 0.40$, $p = 0.05$), in winter ($r^2 = 0.40$, $p = 0.05$), in the Richmond subcatchment ($r^2 = 0.53$, $p = 0.001$), in the Eden subcatchment ($r^2 = 0.60$, $p = 0.001$) and in the Shannonbrook subcatchment ($r^2 = 0.43$, $p = 0.01$). Significant regressions existed for DOC in autumn ($r^2 = 0.69$, $p = 0.001$), in winter ($r^2 = 0.61$, $p = 0.001$), in the Richmond subcatchment ($r^2 = 0.53$, $p = 0.001$), in the Eden subcatchment ($r^2 = 0.74$, $p = 0.001$) and in the Shannonbrook subcatchment ($r^2 = 0.36$, $p = 0.05$). The y-intercepts are colour coded and written in the top left hand corner. There were no significant regressions for CH_4.

1998b). However, despite the higher CH_4 concentrations, the lower transfer velocities during the drier seasons led to lower CH_4 evasion rates. Overall, annual CH_4 evasion was <1% of the total carbon export (Fig. 10). The small contribution of CH_4 to the total carbon export is similar to other riverine systems where this term is generally lower than 1% (Stanley et al., 2015; Striegl et al., 2012).

There was minimal spatial difference in $\delta^{13}C$-CH_4 values between the subcatchments during each season (Fig. 6; Table 3). However,

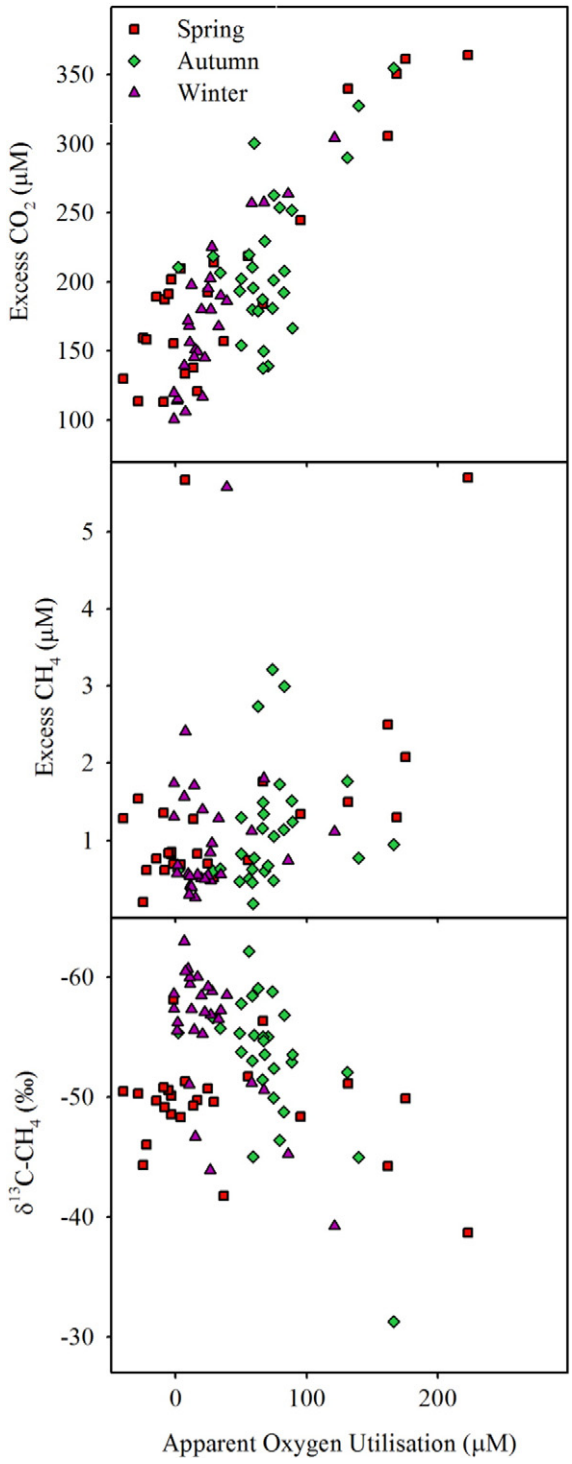

Fig. 8. Scatter plot of apparent oxygen utilisation vs excess CO_2, excess CH_4 and $\delta^{13}C$-CH_4. Note there is no dissolved oxygen data for summer.

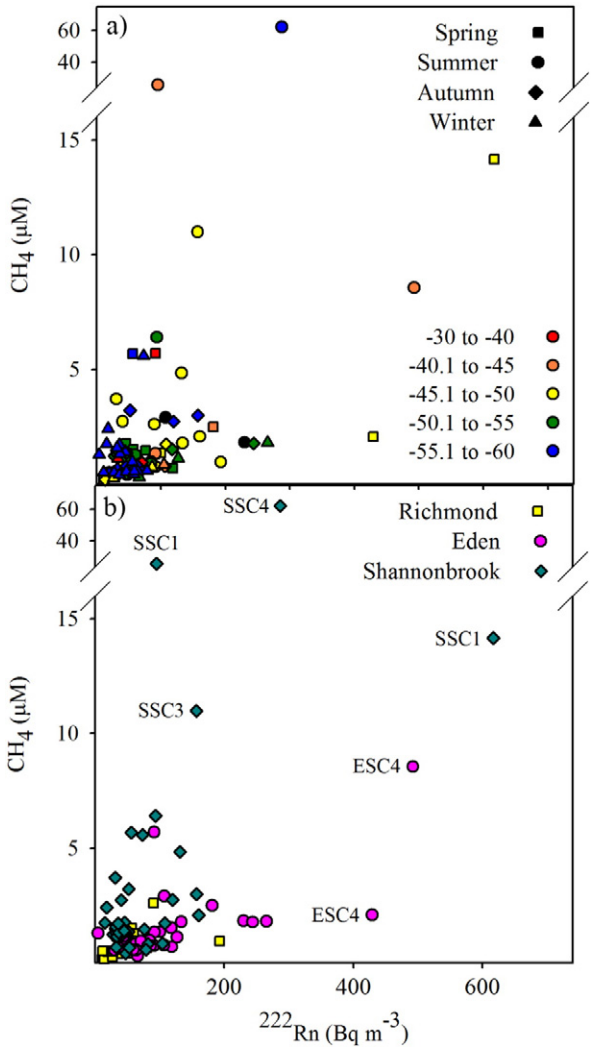

Fig. 9. CH_4 vs radon for a) seasons and b) subcatchments. In plot a) $\delta^{13}C$-CH_4 (‰) is displayed in colour. Labelled sites in plot b) existed as either very slow flowing water or as disconnected pools. These sites had either the highest CH_4 concentrations or the highest radon levels. Overall, CH_4 was significantly correlated to radon ($r^2 = 0.16$, $p < 0.01$). Significant relationships existed for CH_4 and radon during spring ($r^2 = 0.58$, $p < 0.01$), summer ($r^2 = 0.17$, $p = 0.04$) and autumn ($r^2 = 0.25$, $p < 0.01$) but not for winter ($r^2 = 0.02$, $p = 0.52$). Significant relationships existed for CH_4 and radon in the Richmond Subcatchment ($r^2 = 0.2$, $p < 0.01$), the Eden Subcatchment ($r^2 = 0.44$, $p < 0.01$) and the Shannonbrook Subcatchment ($r^2 = 0.24$, $p < 0.01$).

there was a clear seasonal trend where $\delta^{13}C$-CH_4 values were more enriched in the drier season than the wetter seasons (Table 3). During the drier seasons increased CH_4 oxidation in the slow flowing surface water was likely responsible for the enriched CH_4 signal. The more depleted signals for autumn and winter were likely due to the shorter surface water residence times when river discharge was higher, preventing CH_4 oxidation. It was likely $\delta^{13}C$-CH_4 during autumn and winter was more similar to the source signal. Although the Keeling plots (Fig. 7) showed no distinct CH_4 source, the groundwater endmember for $\delta^{13}C$-CH_4 in the Richmond and Eden Subcatchment was -59.07 ± 3.49‰ and for the Shannonbrook Subcatchment were -59.87 ± 7.60‰ (Table 1), implying a combination of oxidised groundwater CH_4 and in situ processes controlling the surface water CH_4 pools.

We found no direct evidence that the presence of CSG exploration wells (now decommissioned) had altered CH_4 dynamics in the creeks investigated. However, because data was not obtained prior to drilling ~50 CSG exploration wells, this can not be confirmed. Our results provide a comparison basis for future impact assessment programs if CSG exploration commences in the region.

5. Conclusions

Hydrology exerted a strong control over carbon exports and evasion rates for each subcatchment. Higher surface water flows and greater precipitation during autumn and winter increased all exported carbon species compared to the drier spring and summer conditions. Groundwater played an important role in delivering DIC, CO_2 and CH_4 to surface waters. DIC export was ~7-fold greater than DOC export during the drier periods, and similar to DOC export during the wetter winter period. DIC

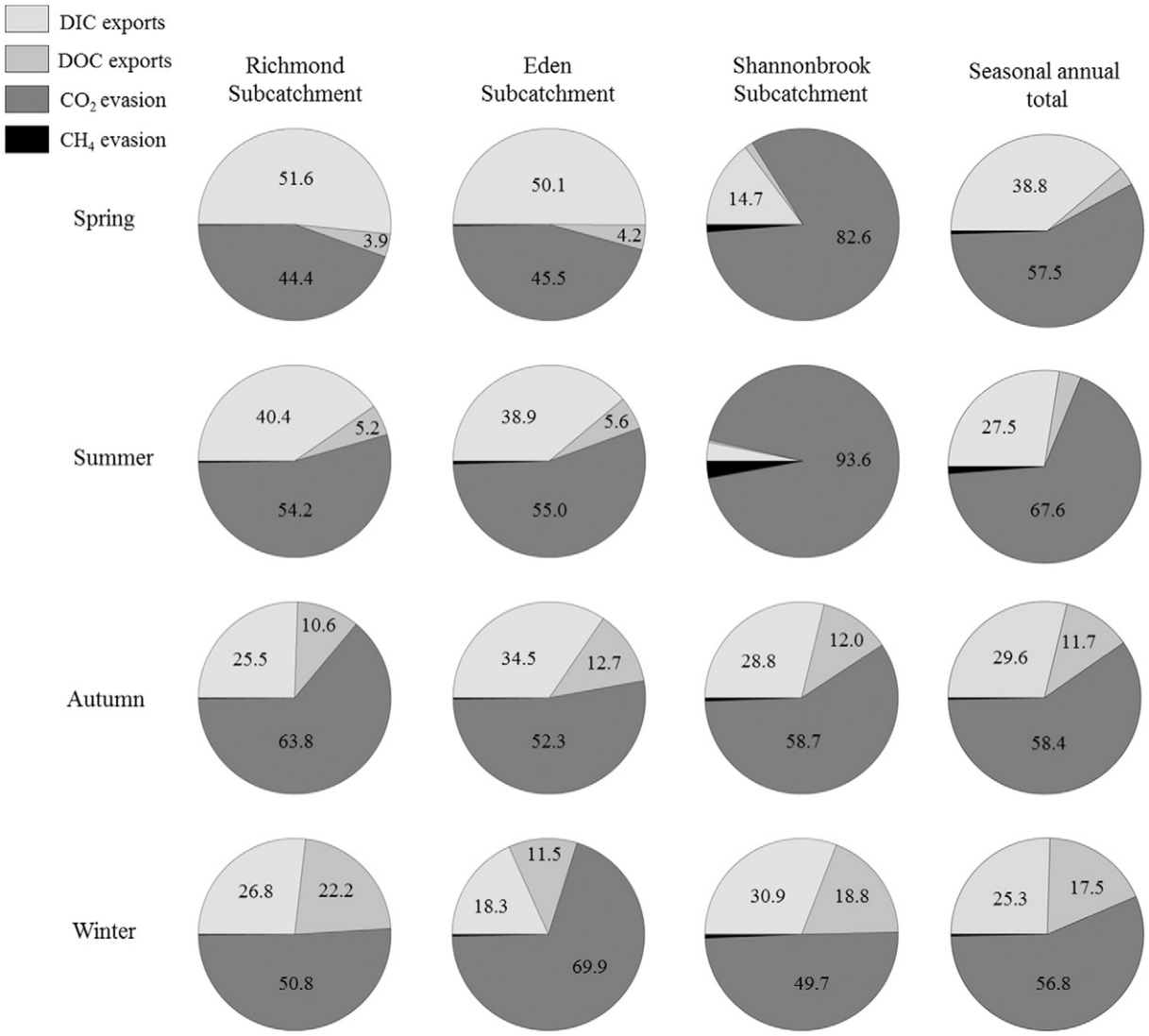

Fig. 10. Pie charts displaying total carbon dynamics for each season (spring, summer autumn and winter) within the Richmond Subcatchment, the Eden Subcatchment and Shannonbrook Subcatchment. Numbers represent percentage values and values below 3% are not numbered. While these values do not represent seasonal changes over an entire year (more sampling campaigns would be necessary), we can make comparisons between warmer drier seasons (spring and summer), and wetter cooler seasons (autumn and winter). Total annual carbon exports were CO_2 (60%), DIC (30%), DOC (9%) and CH_4 (1%) (pie chart not displayed).

exports were highest during winter and were sourced from groundwater inputs and in situ respiration. DOC exports were 1 order of magnitude higher during winter. During autumn and winter, DOC was derived from terrestrial vegetation, and delivered to adjacent surface waters by overland flow. Methane was always supersaturated throughout the seasons, resulting from groundwater discharge and in situ anaerobic processes. Both CO_2 and CH_4 evasion rates were ~2 fold higher in winter compared to spring. Longer surface water residence times in drier conditions likely enhanced CH_4 oxidation.

Riverine carbon dynamics are important when considering the future effects of climate change. Understanding changes associated with hydrology and groundwater discharge will be directly linked to understanding climate change implications. For the subtropical region of the Richmond River Catchment, climate change is expected to reduce average annual rainfall and river discharge, but increase extreme rainfall events (CSIRO, 2007). If hydrological conditions become drier, it is likely DIC/DOC export ratios will reflect those of the spring and summer conditions. The winter conditions in this study reflect a possible response to projected increases in extreme rainfall events, which resulted in flushing soil organic carbon and increased DOC export.

The atmospheric evasion of CO_2, a major greenhouse gas, was the main carbon export pathway (60% of total carbon exports), and investigating CO_2 and other carbon parameters in detail is important when estimating possible riverine climate change feedback mechanisms. Methane evasion accounted for <1% of total carbon exports on a molar basis but is an important parameter because it is a potent greenhouse gas and coal seam gas (a major, unexplored regional resource) is predominantly methane. As such, changes in surface water CH_4 dynamics may provide an early warning for any unconventional gas development impacts.

Acknowledgements

This project was funded by a Northern Rivers Regional Council grant and a Southern Cross University Collaborative Research grant. We thank local landowners for allowing us to take surface water samples from their properties. We would like to thank Anita Perkins, Ben Stewart, Ronny Trnorsky, Sean Madigan, Ceylena Holloway and Douglas Tait for their valuable help during field work. Thanks to Matheus Carvalho for DIC and DOC sample analysis. We acknowledge support from the Australian Research Council (DE140101733, DE150100581, LE120100156 and LP130100498).

Appendix A.

Appendix table
Parameters measured at each site during the four seasons (spring, summer, autumn and winter).

Site	Latitude	Longitude	Date	Temp (°C)(°C)	Sp Cond ($mS\ cm^{-1}$) ($mS\ cm^{-1}$)	pH	DO ($mg\ L^{-1}$) ($mg\ L^{-1}$)	Radon ($Bq\ m^{-3}$) ($Bq\ m^{-3}$)	CH_{4CH4} (μM)(μM)	$\delta^{13}C\text{-}CH_4\delta^{13}$ C-CH_4 (‰)	pCO_2pCO_2 (μatm)(μatm)	DIC (mM)	$\delta^{13}C\text{-}DIC\delta^{13}$ C-DIC (‰)	DOC (mM)	$\delta^{13}C\text{-}DOC\delta^{13}$ C-DOC (‰)	CH_4 evasion CH_4 evasion ($mmol\ m^{-2}\ d^{-1}$) ($mmol\ m^{-2}\ d^{-1}$)	CO_2 evasion CO_2 evasion ($mmol\ m^{-2}\ d^{-1}$) ($mmol\ m^{-2}\ d^{-1}$)
Spring																	
RSC1	−28.56603	152.97575	10/16/2013	20.90	0.33	7.82	7.16	75.1	0.75	−51.69	6148	2.27	−9.81	0.18	−27.56	0.49	161.54
RSC2	−28.61668	153.00257	10/16/2013	17.30	0.47	7.48	5.38	56.9	1.50	−51.13	8424	4.08	−10.78	0.32	−27.01	1.29	316.34
RSC3	−28.6208	152.99532	10/16/2013	20.20	0.34	7.75	8.12	24.3	0.53	−49.61	5910	2.57	−9.79	0.21	−27.09	0.74	320.89
RSC4	−28.67927	152.9984	10/16/2013	24.40	0.36	8.04	8.22	53.2	0.69	−48.31	6485	2.72	−9.62	0.20	−26.14	0.52	176.87
RSC5	−28.74185	152.97785	10/16/2013	24.50	0.38	7.93	8.43	44.9	0.82	−50.12	6274	2.84	−9.48	0.20	−26.85	0.62	172.07
RSC6	−28.78381	152.97529	10/16/2013	25.80	0.39	7.99	8.61	54.2	0.76	−49.67	6095	2.95	−9.46	0.22	−26.68	1.18	310.27
RSC7	−28.84103	152.97957	10/16/2013	24.70	0.42	8.02	8.40	62.1	0.85	−48.53	6301	2.94	−9.15	0.23	−26.84	0.68	180.74
RSC8	−28.86859	153.04449	10/17/2013	26.00	0.43	8.19	8.90	10.9	0.20	−44.33	5232	3.01	−8.09	0.24	−27.76	0.16	134.24
RSC9	−28.88618	153.12514	10/17/2013	27.30	0.46	8.13	8.63	45.7	0.61	−46.00	5361	3.06	−8.14	0.23	−27.05	0.54	141.69
ESC1	−28.66177	152.91624	10/16/2013	19.50	0.51	8.05	6.12	100.2	1.35	−48.33	6574	4.05	−9.30	0.30	−27.50	1.13	224.80
ESC2	−28.66315	152.90122	10/16/2013	21.40	0.28	7.93	8.06	118.6	0.70	−50.69	5530	1.84	−9.83	0.29	−27.50	1.44	413.68
ESC3	−28.71397	152.90556	10/16/2013	20.00	1.11	7.73	3.45	429.5	2.08	−49.85	9670	7.17	−9.00	0.47	−26.27	1.82	345.61
ESC4	−28.71568	152.86027	10/16/2013	23.10	0.39	8.22	8.82	43.4	0.62	−49.15	5645	2.62	−9.18	0.27	−26.98	0.88	284.09
ESC5	−28.74397	152.9131	10/16/2013	20.80	0.94	7.83	3.75	181.1	2.50	−44.21	8419	6.37	−9.37	0.52	−25.07	2.32	308.31
ESC6	−28.75749	152.92398	10/16/2013	22.60	0.42	8.15	8.81	57.1	0.84	−50.55	5680	3.01	−8.75	0.28	−26.73	1.29	310.78
ESC7	−28.81236	152.90164	10/16/2013	20.90	0.80	7.55	3.51	90.0	1.30	x	9622	5.39	−8.42	0.56	−23.67	0.93	278.09
ESC8	−28.80243	152.93706	10/16/2013	19.60	0.98	7.45	2.01	91.3	5.70	−38.68	9626	5.27	−9.15	0.75	−23.89	3.31	239.95
ESC9	−28.80402	152.95439	10/16/2013	27.30	0.44	8.10	7.97	37.5	0.70	−58.13	5271	3.01	−8.92	0.25	−26.18	1.30	306.82
SSC1	−28.90516	152.8782	10/17/2013	22.20	0.44	7.17	x	617.0	14.16	−46.67	10625	3.27	−8.52	0.18	−24.67	4.19	116.99
SSC3	−28.97926	152.90512	10/17/2013	24.50	0.30	7.45	8.10	76.6	1.47	−51.30	4285	1.09	−8.51	0.25	−27.67	2.39	220.16
SSC4	−28.94683	152.97314	10/17/2013	23.50	0.33	7.20	6.35	56.1	5.68	−56.33	5613	1.29	−11.42	0.30	−27.93	7.48	245.99
SSC5	−28.86748	152.9114	10/17/2013	18.30	1.26	8.09	8.85	81.9	0.83	−49.73	3347	4.85	−6.76	0.25	−24.56	2.24	329.64
SSC6	−28.92302	152.97397	10/17/2013	20.00	1.39	7.98	8.62	43.2	1.28	−49.29	3938	5.19	−7.58	0.39	−26.03	2.29	249.32
SSC7	−28.93158	153.00479	10/17/2013	26.40	1.13	7.83	9.31	45.9	1.77	−50.47	4385	3.74	−8.30	0.34	−25.88	1.51	114.01
SSC8	−28.94349	153.06176	10/17/2013	27.30	1.13	7.96	8.19	31.3	1.29	−50.79	3952	3.81	−8.75	0.39	−26.67	0.59	54.26
SSC9	−28.92177	153.11228	10/17/2013	25.50	1.18	7.98	9.08	51.5	1.36	−50.26	3804	3.55	−8.89	0.42	−26.41	2.23	188.84
SSC10	−28.92701	153.15788	10/17/2013	25.50	0.89	7.72	7.00	41.4	1.55	−41.74	5102	3.49	−8.81	0.33	−26.29	1.75	181.03
Summer																	
RSC1	−28.56603	152.97575	2/11/2014	24.97	0.23	7.56	x	60.0	1.27	−52.18	5806	1.76	−8.34	0.24	−25.13	2.03	295.80
RSC2	−28.61668	153.00257	2/11/2014	21.65	0.35	7.74	x	90.0	2.61	−47.46	7319	2.92	−9.39	0.36	−25.21	2.94	293.16
RSC3	−28.6208	152.99532	2/11/2014	24.62	0.27	7.96	x	79.6	0.65	−46.91	5631	1.90	−7.95	0.25	−24.84	1.04	288.73
RSC4	−28.67927	152.9984	2/11/2014	25.13	0.30	7.97	x	77.5	0.72	−46.28	5916	2.07	−7.28	0.26	−24.50	0.73	192.61
RSC5	−28.74185	152.97785	2/11/2014	27.14	0.32	8.04	x	193.0	0.96	−48.27	6278	2.13	−7.10	0.27	−24.47	0.98	197.35
RSC6	−28.78381	152.97529	2/11/2014	27.65	0.32	8.03	x	84.8	0.88	−52.95	6420	2.17	−7.26	0.25	−24.56	1.31	287.89
RSC7	−28.84103	152.97957	2/11/2014	28.82	0.37	7.97	x	41.2	0.96	−45.26	5815	2.39	−7.21	0.29	−24.79	0.97	170.00
RSC8	−28.86859	153.04449	2/12/2014	24.75	0.40	7.88	x	19.9	0.51	−40.63	5203	2.51	−6.75	0.34	−25.58	0.59	194.35
RSC9	−28.88618	153.12514	2/12/2014	27.79	0.44	8.01	x	51.0	1.29	−44.93	5999	2.72	−6.92	0.35	−25.52	1.73	240.64
ESC1	−28.66177	152.91624	2/11/2014	23.45	0.47	7.89	x	91.6	1.33	−44.01	5806	2.75	−7.71	0.43	−24.52	1.67	242.75
ESC2	−28.66315	152.90122	2/11/2014	24.92	0.25	7.89	x	133.5	1.78	−46.81	5678	1.40	−7.42	0.37	−25.15	3.32	338.20
ESC3	−28.71397	152.90556	2/11/2014	23.99	1.20	7.61	x	492.5	8.55	−44.76	9425	7.07	−7.87	0.75	−20.82	13.72	507.81
ESC4	−28.71568	152.86027	2/11/2014	25.65	0.35	7.97	x	91.2	0.75	−46.39	5216	2.08	−7.68	0.38	−24.59	1.31	281.80
ESC5	−28.74397	152.9131	2/11/2014	23.49	0.90	7.64	x	229.7	1.82	x	8656	5.06	−7.11	0.73	−22.20	1.32	214.95
ESC6	−28.75749	152.92398	2/11/2014	26.92	0.38	8.02	x	84.5	0.97	−48.94	5340	2.15	−7.04	0.35	−24.36	1.82	299.98
ESC7	−28.81236	152.90164	2/11/2014	22.69	0.68	7.14	x	107.1	2.91	x	11402	4.00	−8.38	0.90	−23.54	2.59	359.11
ESC9	−28.80402	152.95439	2/11/2014	28.95	0.41	8.29	x	30.3	0.54	−50.63	5089	2.26	−7.10	0.32	−24.45	0.85	227.09
SSC1	−28.90516	152.8782	2/12/2014	20.32	0.46	7.40	x	95.1	25.53	−42.30	15566	3.86	−5.90	0.41	−24.21	18.17	422.81
SSC3	−28.97926	152.90512	2/12/2014	23.35	0.37	7.24	x	156.9	10.99	−49.86	7157	1.47	−10.43	0.26	−24.96	8.99	198.87
SSC4	−28.94683	152.97314	2/12/2014	21.23	0.41	6.66	x	287.2	62.13	−58.14	19919	1.89	−9.09	0.36	−24.72	47.91	574.49
SSC5	−28.86748	152.9114	2/12/2014	20.27	1.16	7.97	x	160.6	2.08	−47.71	4252	4.21	−7.24	0.31	−22.20	4.51	325.25
SSC6	−28.92302	152.97397	2/12/2014	20.50	1.42	7.87	x	131.9	4.85	−46.90	5159	4.77	−8.13	0.49	−22.24	9.43	357.66
SSC7	−28.93158	153.00479	2/12/2014	24.29	1.31	7.15	x	93.8	6.40	−50.92	5866	4.13	−8.30	0.46	−22.82	6.42	191.68
SSC8	−28.94349	153.06176	2/12/2014	26.61	1.28	7.78	x	40.5	2.73	−48.54	3782	3.49	−7.87	0.47	−23.30	2.21	90.32

(continued on next page)

Appendix table (*continued*)

Site	Latitude	Longitude	Date	Temp (°C)(°C)	Sp Cond ($mS\ cm^{-1}$) ($mS\ cm^{-1}$)	pH	DO ($mg\ L^{-1}$) ($mg\ L^{-1}$)	Radon ($Bq\ m^{-3}$) ($Bq\ m^{-3}$)	CH_{4CH4} (μM)(μM)	$\delta^{13}C\text{-}CH_4\delta^{13}$ C-CH_4 (‰)	pCO_2pCO_2 (μatm)(μatm)	DIC (mM)	$\delta^{13}C\text{-}DIC\delta^{13}$ C-DIC (‰)	DOC (mM)	$\delta^{13}C\text{-}DOC\delta^{13}$ C-DOC (‰)	CH_4 evasion CH_4 evasion ($mmol\ m^{-2}\ d^{-1}$) ($mmol\ m^{-2}\ d^{-1}$)	CO_2 evasion CO_2 evasion ($mmol\ m^{-2}\ d^{-1}$) ($mmol\ m^{-2}\ d^{-1}$)
SSC9	−28.92177	153.11228	2/12/2014	25.34	1.39	7.73	x	31.1	3.71	−49.28	4672	3.42	−8.20	0.47	−23.68	7.62	296.50
SSC10	−28.92701	153.15788	2/12/2014	25.12	0.57	7.85	x	47.6	0.42	−34.01	6843	3.09	−7.02	0.38	−24.96	0.51	271.76
Autumn																	
RSC1	−28.56603	152.97575	5/7/2014	15.08	0.41	6.73	8.26	63.8	0.51	−62.11	5250	1.43	−8.01	0.29	−25.97	0.71	311.85
RSC2	−28.61668	153.00257	5/7/2014	13.72	0.22	7.09	8.44	46.2	0.77	−55.15	6735	1.44	−4.75	0.47	−24.43	1.76	688.38
RSC3	−28.6208	152.99532	5/7/2014	15.24	0.28	7.54	8.46	32.7	0.47	−55.31	4685	1.66	−7.74	0.34	−25.36	0.75	310.72
RSC4	−28.67927	152.9984	5/7/2014	15.53	0.29	7.66	8.09	46.9	0.46	−53.00	5109	0.85	−3.65	0.35	−24.30	0.55	255.20
RSC5	−28.74185	152.97785	5/7/2014	16.85	0.28	7.73	9.62	50.7	0.61	−55.34	5306	1.42	−4.54	0.34	−24.02	0.65	225.78
RSC6	−28.78381	152.97529	5/7/2014	17.30	0.25	7.48	8.68	34.9	0.61	−56.59	5559	0.85	−5.78	0.30	−23.81	0.97	352.85
RSC7	−28.84103	152.97957	5/7/2014	16.94	0.29	7.34	7.49	49.6	0.61	−53.53	5760	1.82	−4.11	0.33	−23.42	0.54	206.97
RSC8	−28.86859	153.04449	5/8/2014	17.65	0.32	7.63	7.63	13.8	0.19	−45.01	5074	1.77	−3.09	0.31	−23.60	0.18	193.37
RSC9	−28.88618	153.12514	5/8/2014	18.59	0.33	7.78	6.95	36.2	0.48	−49.91	5344	0.77	−3.84	0.32	−23.78	0.75	314.62
ESC1	−28.66177	152.91624	5/7/2014	14.55	0.42	7.72	7.77	46.0	1.06	−52.39	6095	2.81	−8.57	0.33	−25.19	1.46	365.56
ESC2	−28.66315	152.90122	5/7/2014	15.60	0.34	7.74	7.82	44.7	1.16	−51.42	4602	1.31	−2.55	0.40	−26.05	1.66	271.23
ESC3	−28.71397	152.90556	5/7/2014	14.63	0.77	7.52	5.95	243.9	1.77	−52.06	6709	2.20	−6.60	1.14	−21.00	3.63	596.32
ESC4	−28.71568	152.86027	5/7/2014	15.46	0.38	7.64	8.88	67.4	0.64	−55.72	5008	1.50	−5.28	0.38	−24.63	0.96	314.35
ESC5	−28.74397	152.9131	5/7/2014	14.52	0.64	7.40	7.33	117.5	1.52	−52.90	5856	2.87	−8.53	0.97	−20.91	1.48	248.05
ESC6	−28.75749	152.92398	5/7/2014	16.07	0.42	7.66	8.24	62.6	0.83	−57.76	5000	2.10	−6.53	0.44	−23.38	1.12	274.45
ESC7	−28.81236	152.90164	5/7/2014	16.41	0.40	7.05	4.45	70.9	0.95	−31.28	8549	0.60	−1.19	1.50	−19.99	0.81	308.32
ESC8	−28.80243	152.93706	5/7/2014	15.86	0.47	7.56	5.42	106.4	0.78	−44.97	7798	0.90	−7.83	1.72	−20.68	0.57	243.68
ESC9	−28.80402	152.95439	5/7/2014	17.31	0.42	7.70	7.72	51.5	0.63	−58.40	4650	1.47	−6.90	0.54	−22.82	0.89	257.41
SSC1	−28.90516	152.8782	5/8/2014	14.69	0.56	7.60	7.59	108.2	1.73	−46.40	5931	3.55	−7.02	0.45	−25.24	1.08	160.03
SSC2	−28.9526	152.92583	5/8/2014	16.40	0.33	7.43	7.12	157.3	3.00	−56.79	5179	2.39	−7.97	0.40	−23.55	5.30	369.79
SSC3	−28.97926	152.90512	5/8/2014	15.89	0.26	7.35	7.87	119.8	2.74	−59.03	4448	0.30	−1.50	0.50	−24.19	5.51	361.96
SSC4	−28.94683	152.97314	5/8/2014	16.17	0.28	7.31	7.46	52.2	3.22	−58.77	4532	0.59	−2.17	0.45	−23.72	4.61	261.21
SSC5	−28.86748	152.9114	5/8/2014	15.60	1.16	7.81	7.66	53.0	0.68	−55.01	3521	1.55	−5.81	0.65	−21.69	2.12	438.92
SSC6	−28.92302	152.97397	5/8/2014	15.62	1.18	7.90	7.78	31.6	1.49	−55.00	3488	2.14	−4.36	0.59	−21.18	2.92	269.77

SSC7	−28.93158	153.00479	5/8/2014	16.14	0.81	7.40	7.67	46.6	1.35	−54.71	3821	2.13	−5.43	0.54	−21.97	1.75	196.15
SSC8	−28.94349	153.06176	5/8/2014	16.10	0.78	7.73	6.97	28.0	1.24	−53.53	4196	1.38	−6.59	0.58	−21.99	1.31	177.15
SSC9	−28.92177	153.11228	5/8/2014	16.69	0.77	7.69	8.10	32.7	1.30	−53.76	3977	1.24	−6.29	0.59	−21.91	3.13	372.94
SSC10	−28.92701	153.15788	5/8/2014	15.69	0.75	7.48	7.27	33.4	1.14	−48.75	4729	1.51	−6.11	0.63	−21.90	2.15	363.41
Winter																	
RSC1	−28.56603	152.97575	9/2/2014	17.18	0.23	6.85	9.27	58.2	0.42	−59.39	x	0.95	−5.39	0.38	−25.75	0.91	x
RSC2	−28.61668	153.00257	9/2/2014	15.28	0.20	7.03	9.13	55.6	0.97	−58.82	5398	0.70	−3.94	0.26	−25.33	2.85	667.19
RSC3	−28.6208	152.99532	9/2/2014	16.50	0.23	7.28	9.37	35.5	0.40	−57.29	4957	0.82	−4.55	0.39	−25.67	1.44	718.30
RSC4	−28.67927	152.9984	9/2/2014	16.10	0.21	7.09	8.99	19.8	0.48	−56.85	4494	0.86	−4.29	0.50	−25.25	1.47	553.68
RSC5	−28.74185	152.97785	9/2/2014	17.73	0.23	6.47	8.72	63.2	0.55	−59.18	5073	1.11	−6.82	0.62	−22.94	1.24	445.02
RSC6	−28.78381	152.97529	9/2/2014	17.60	0.22	6.23	8.91	11.3	0.51	−58.44	4690	0.90	−5.03	0.68	−22.83	1.32	470.13
RSC7	−28.84103	152.97957	9/2/2014	17.50	0.24	6.70	8.46	55.0	0.56	−57.19	4919	0.86	−4.65	0.73	−23.30	0.87	300.29
RSC8	−28.86859	153.04449	9/3/2014	16.00	0.21	7.00	9.38	26.4	0.26	−46.69	3827	0.70	−5.21	0.83	−23.21	0.65	383.69
RSC9	−28.88618	153.12514	9/3/2014	17.14	0.22	6.94	8.92	27.5	0.50	−57.05	3812	0.97	−7.96	0.80	−23.19	1.25	365.31
ESC1	−28.66177	152.91624	9/2/2014	15.73	0.31	6.92	8.87	4.5	1.29	−56.48	4178	1.28	−6.09	0.59	−24.96	3.74	491.85
ESC2	−28.66315	152.90122	9/2/2014	16.16	0.25	7.17	9.50	66.0	0.30	−51.05	4241	0.91	−4.09	0.44	−26.31	1.48	839.14
ESC3	−28.71397	152.90556	9/2/2014	15.40	0.53	6.77	7.82	265.6	1.81	−50.58	6138	1.77	−7.49	1.23	−20.41	16.92	2421.87
ESC4	−28.71568	152.86027	9/2/2014	16.77	0.27	7.14	9.17	63.8	0.56	−60.00	3877	1.07	−4.70	0.61	−25.10	2.24	607.58
ESC5	−28.74397	152.9131	9/2/2014	15.23	0.53	6.63	8.16	126.8	1.12	−51.17	6094	2.27	−7.59	1.10	−20.49	6.47	1488.16
ESC6	−28.75749	152.92398	9/2/2014	17.48	0.30	6.79	9.26	58.7	0.57	−60.66	4486	1.18	−4.51	0.62	−24.27	2.16	659.09
ESC7	−28.81236	152.90164	9/2/2014	15.75	0.30	6.37	6.04	33.6	1.12	−39.22	7243	1.09	−6.59	1.30	−21.40	1.63	449.47
ESC8	−28.80243	152.93706	9/2/2014	16.72	0.30	6.27	6.97	85.9	0.74	−45.24	6515	0.90	−6.64	1.63	−20.53	1.30	466.73
ESC9	−28.80402	152.95439	9/2/2014	18.56	0.30	7.15	9.00	46.8	0.54	−59.95	4231	1.09	−4.11	0.69	−23.72	1.78	518.15
SSC1	−28.90516	152.8782	9/3/2014	15.12	0.45	7.60	9.20	104.4	0.85	−43.89	4875	2.12	−7.29	0.55	−25.17	1.21	292.82
SSC2	−28.9526	152.92583	9/3/2014	14.35	0.29	6.93	10.01	32.3	1.57	−62.96	3406	0.78	−3.34	0.57	−22.54	4.71	421.45
SSC3	−28.97926	152.90512	9/3/2014	16.40	0.26	7.13	9.82	15.4	1.74	−58.58	2716	0.64	−3.25	0.53	−24.33	4.64	270.27
SSC4	−28.94683	152.97314	9/3/2014	16.79	0.27	7.40	9.46	18.1	2.41	−60.45	2870	0.64	−5.29	0.73	−23.56	5.75	255.01
SSC5	−28.86748	152.9114	9/3/2014	13.83	0.87	7.42	10.28	78.8	0.58	−55.50	2825	3.11	−6.01	0.59	−22.79	2.38	475.57
SSC6	−28.92302	152.97397	9/3/2014	14.07	0.84	7.59	10.21	32.8	0.68	−56.19	2863	2.80	−5.37	0.58	−22.17	1.76	299.24
SSC7	−28.93158	153.00479	9/3/2014	15.11	0.63	6.93	10.08	36.8	1.31	−57.34	3045	2.13	−6.80	0.67	−22.61	2.81	258.33
SSC8	−28.94349	153.06176	9/3/2014	16.45	0.54	7.22	9.10	45.2	1.40	−55.24	3093	1.66	−7.01	0.81	−22.22	2.81	236.60
SSC9	−28.92177	153.11228	9/3/2014	16.00	0.52	6.89	9.40	35.6	1.71	−55.58	3709	1.53	−6.10	0.80	−22.30	5.70	487.71
SSC10	−28.92701	153.15788	9/3/2014	16.71	0.49	6.77	8.46	73.5	5.58	−58.50	4718	1.29	−6.26	0.79	−22.34	11.47	384.99

References

Abril, G., Etcheber, H., Borges, A.V., Frankignoulle, M., 2000. Excess atmospheric carbon dioxide transported by rivers into the Scheldt estuary. C.R. Acad. Sci. Ser. IIA Earth Planet. Sci. 330 (11), 761–768.

Abril, G., Commarieu, M.V., Guérin, F., 2007. Enhanced methane oxidation in an estuarine turbidity maximum. Limnol. Oceanogr. 52 (1), 470–475.

Adrian, N.R., Robinson, J.A., Suflita, J.M., 1994. Spatial variability in biodegradation rates as evidenced by methane production from an aquifer. Appl. Environ. Microbiol. 60 (10), 3632–3639.

Amon, R., Benner, R., 1996. Photochemical and microbial consumption of dissolved organic carbon and dissolved oxygen in the Amazon River system. Geochim. Cosmochim. Acta 60, 1783–1792.

Anthony, S.E., Prahl, F.G., Peterson, T.D., 2012. Methane dynamics in the Willamette River, Oregon. Limnol. Oceanogr. 57 (5), 1517–1530.

Apte, S., McCabe, P., Oliver, R., Paterson, L., 2014. Condamine River Gas Seeps Investigations: Independent Review. Department of Natural Resources and Management, Queensland.

Aravena, R., Suzuki, O., 1990. Isotopic evolution of river water in the northern Chile region. Water Resour. Res. 26 (12), 2887–2895.

Atekwana, E.A., Krishnamurthy, R.V., 1998. Seasonal variations of dissolved inorganic carbon and $\delta^{13}C$ of surface waters: application of a modified gas evolution technique. J. Hydrol. 205, 265–278.

Atkins, M.L., Santos, I.R., Ruiz-Halpern, S., Maher, D.T., 2013. Carbon dioxide dynamics driven by groundwater discharge in a coastal floodplain creek. J. Hydrol. 493, 30–42.

Atkins, M.L., Santos, I.R., Maher, D.T., 2015. Groundwater methane in a potential coal seam gas extraction region. J. Hydrol. Reg. Stud. 4, 452–471.

Atkins, M.L., Santos, I.R., Maher, D.T., 2016a. Assessing groundwater-surface water connectivity using radon and major ions prior to coal seam gas development (Richmond River Catchment, Australia). Applied Geochemistry (Article in press).

Atkins, M.L., Santos, I.R., Perkins, A.K., Maher, D.T., 2016b. Dissolved radon and uranium in groundwater in a potential coal seam gas development region (Richmond River Catchment, Australia). J. Environ. Radioact. 154, 83–92.

Aucour, A.-M., Sheppard, S.M.F., Guyomar, O., Wattelet, J., 1999. Use of ^{13}C to trace origin and cycling of inorganic carbon in the Rhone river system. Chem. Geol. 159, 87–105.

Avery, G.B., Willey, J.D., Kieber, R.J., Shank, G.C., Whitehead, R.F., 2003. Flux and bioavailability of Cape Fear River and rainwater dissolved organic carbon to Long Bay, southeastern United States. Glob. Biogeochem. Cycles 17 (2).

Barth, J.A.C., Cronin, A.A., Dunlop, J., Kalin, R.M., 2003. Influence of carbonates on the riverine carbon cycle in an anthropogenically dominated catchment basin: evidence from major elements and stable carbon isotopes in the Lagan River (N. Ireland). Chem. Geol. 200 (3–4), 203–216.

Benner, R., Opsahl, S., 2001. Molecular indicators of the sources and transformations of dissolved organic matter in the Mississippi River plume. Org. Geochem. 32, 597–611.

Benson, B.B., Krause, D., 1984. The concentration and isotopic fractionation of oxygen dissolved in freshwater and seawater in equilibrium with the atmosphere. Limnol. Oceanogr. 29, 620–632.

Bergman, I., Klarqvist, M., Nilsson, M., 2000. Seasonal variation in rates of methane production from peat of various botanical origins: effects of temperature and substrate quality. FEMS Microbiol. Ecol. 33 (3), 181–189.

BOM, 2014. Australian Government, Bureau of Meterology. Retrieved from www.bom.gov.au.

Borges, A., Abril, G., 2011. Carbon dioxide and methane dynamics in estuaries. Treatise on Estuarine and Coastal Science, 5: Biogeochemistry. Academic Press, Waltham.

Borges, A.V., Vanderborght, J.-P., Schiettecatte, L.-S., Gazeau, F., Ferron-Smith, S., Delille, B., Frankignoulle, M., 2004. Variability of the gas transfer velocity of CO_2 in a macrotidal estuary (the Scheldt). Estuaries 27 (4), 593–603.

Borges, A.V., Darchambeau, F., Teodoru, C.R., Marwick, T.R., Tamooh, F., Geeraert, N., Omengo, F.O., Guerin, F., Lambert, T., Morana, C., Okuku, E., Bouillon, S., 2015. Globally significant greenhouse-gas emissions from African inland waters. Nat. Geosci. 8 (8), 637–642.

Buhl, D., Neuser, R.D., Richter, D.K., Riedel, D., Roberts, B., Strauss, H., Veizer, J., 1991. Nature and nurture: environmental isotope story of the river Rhine. Naturwissenschaften 78, 337–346.

Burnett, W.C., Kim, G., Lane-Smith, D., 2001. A continuous monitor for assessment of ^{222}Rn in the coastal ocean. J. Radioanal. Nucl. Chem. 249 (1), 167–172.

Cai, Y., Guo, L., Douglas, T.A., 2008. Temporal variations in organic carbon species and fluxes from the Chena River, Alaska. Limnol. Oceanogr. 53 (4), 1408–1419.

Call, M., Maher, D.T., Santos, I.R., Ruiz-Halpern, S., Mangion, P., Sanders, C.J., Erler, D.V., Oakes, J.M., Rosentreter, J., Murray, R., Eyre, B.D., 2015. Spatial and temporal variability of carbon dioxide and methane fluxes over semi-diurnal and spring–neap–spring timescales in a mangrove creek. Geochim. Cosmochim. Acta 150, 211–225.

Campeau, A., Del Giorgio, P.A., 2014. Patterns in CH_4 and CO_2 concentrations across boreal rivers: major drivers and implications for fluvial greenhouse emissions under climate change scenarios. Glob. Chang. Biol. 20 (4), 1075–1088.

Cole, J., Prairie, Y., Caraco, N., McDowell, W., Tranvik, L., Striegl, R., Duarte, C., Kortelainen, P., Downing, J., Middelburg, J., Melack, J., 2007. Plumbing the global carbon cycle: integrating inland waters into the terrestrial carbon budget. Ecosystems 10 (1), 172–185.

Crawford, J.T., Stanley, E.H., 2015. Controls on methane concentrations and fluxes in streams draining human-dominated landscapes. Ecological Applications.

Crosson, E.R., 2008. A cavity ring-down analyzer for measuring atmospheric levels of methane, carbon dioxide, and water vapor. Appl. Phys. B Lasers Opt. 92 (3), 403–408.

CSIRO, 2007. Climate Change in the Northern Rivers Catchment. New South Wales Government. Retrieved from http://trove.nla.gov.au/work/35244494?selectedversion=NBD42807044.

Dalzell, B.J., King, J.Y., Mulla, D.J., Finlay, J.C., Sands, G.R., 2011. Influence of subsurface drainage on quantity and quality of dissolved organic matter export from agricultural landscapes. J. Geophys. Res. Biogeosci. 116 (2).

de Angelis, M.A., Lilley, M.D., 1987. Methane in surface waters of Oregon estuaries and rivers. Limnol. Oceanogr. 32 (3), 716–722.

de Angelis, M.A., Scranton, M.I., 1993. Fate of methane in the Hudson River and Estuary. Glob. Biogeochem. Cycles 7 (3), 509–523.

De Fátima, F.L., Rasera, M., Victoria, R., Ballester, M., Krusche, A.V., Salimon, C., Montebelo, L.A., Alin, S.R., Victoria, R.L., Richey, J.E., 2008. Estimating the surface area of small rivers in the southwestern amazon and their role in CO_2 outgassing. Earth Interact. 12 (6).

de Weys, J., Santos, I.R., Eyre, B.D., 2011. Linking groundwater discharge to severe estuarine acidification during a flood in a modified wetland. Environ. Sci. Technol. 45 (8), 3310–3316.

DelSontro, T., McGinnis, D.F., Sobek, S., Ostrovsky, I., Wehrli, B., 2010. Extreme methane emissions from a swiss hydropower reservoir: contribution from bubbling sediments. Environ. Sci. Technol. 44, 2419–2425.

Dickson, A.G., Millero, F.J., 1987. A comparison of the equilibrium constants for the dissociation of carbonic acid in seawater media. Deep Sea Res. Part A 34 (10), 1733–1743.

DPI, 2012. The Richmond Catchment. Department of Primary Industries, NSW Office of Water. Retrieved from http://www.water.nsw.gov.au/Water-management/Basins-and-catchments/Richmond-catchment/Richmond-catchment.

Drury, L.W., 1982. Hydrogeology and Quaternary Stratigraphy of the Richmond River Valley, New South Wales PhD Thesis University of New South Wales, NSW.

Flintrop, C., Hohlmann, B., Jasper, T., Korte, C., Podlaha, O., Scheele, S.M., Veizer, J., 1996. Anatomy of pollution: rivers of North – Rhine – Westphalia, Germany. Am. J. Sci. 296, 59–98.

Garnier, J., Vilain, G., Silvestre, M., Billen, G., Jehanno, S., Poirier, D., Martinez, A., Decuq, C., Cellier, P., Abril, G., 2013. Budget of methane emissions from soils, livestock and the river network at the regional scale of the Seine basin (France). Biogeochemistry 116 (1–3), 199–214.

Gatland, J., Santos, I.R., Maher, D.T., Dubcan, T.M., Erler, D.V., 2014. Carbon dioxide and methane emissions from an artificially drained coastal wetland during a flood: implications for wetland global warming potential. J. Geophys. Res. Biogeosci. 119 (8), 1698–1716.

Griffiths, N.A., Tank, J.L., Royer, T.V., Warrner, T.J., Frauendorf, T.C., Rosi-Marshall, E.J., Whiles, M.R., 2012. Temporal variation in organic carbon spiraling in Midwestern agricultural streams. Biogeochemistry 108 (1–3), 149–169.

Hanley, K.W., Wollheim, W.M., Salisbury, J., Huntington, T., Aiken, G., 2013. Controls on dissolved organic carbon quantity and chemical character in temperate rivers of North America. Glob. Biogeochem. Cycles 27 (2), 492–504.

Heffernan, J.B., Sponseller, R.A., Fisher, S.G., 2008. Consequences of a biogeomorphic regime shift for the hyporheic zone of a Sonoran Desert stream. Freshw. Biol. 53 (10), 1954–1968.

Helie, J.-F., Hillaire-Marcel, C., Rondeau, B., 2002. Seasonal changes in the sources and fluxes of dissolved inorganic carbon through the St. Lawrence River—isotopic and chemical constraint. Chem. Geol. 186, 117–138.

Ho, D.T., Coffineau, N., Hickman, B., Chow, N., Koffman, T., Schlosser, P., 2016. Influence of current velocity and wind speed on air-water gas exchange in a mangrove estuary. Geophys. Res. Lett.

Hope, D., Billet, M.F., Cresser, M.S., 1994. A review of the export of carbon in river water: fluxes and processes. Environ. Pollut. 84, 301–324.

Hope, D., Palmer, S.M., Billett, M.F., Dawson, J.J.C., 2001. Carbon dioxide and methane evasion from a temperate peatland stream. Limnol. Oceanogr. 46 (4), 847–857.

Hossler, K., Bauer, J.E., 2013. Amounts, isotopic character, and ages of organic and inorganic carbon exported from rivers to ocean margins: 2. Assessment of natural and anthropogenic controls. Glob. Biogeochem. Cycles 27, 347–362.

Hrachowitz, M., Bohte, R., Mul, M.L., Bogaard, T.A., Savenije, H.H.G., Uhlenbrook, S., 2011. On the value of combined event runoff and tracer analysis to improve understanding of catchment functioning in a data-scarce semi-arid area. Hydrol. Earth Syst. Sci. 15 (6), 2007–2024.

Huang, T.-H., Fu, Y.-H., Pan, P.-Y., Chen, C.-T.A., 2012. Fluvial carbon fluxes in tropical rivers. Curr. Opin. Environ. Sustain. 4, 162–169.

Huntington, T.G., Aiken, G.R., 2013. Export of dissolved organic carbon from the Penobscot River basin in north-central Maine. J. Hydrol. 476, 244–256.

Iverach, C.P., Cendón, D.I., Hankin, S.I., Lowry, D., Fisher, R.E., France, J.L., Nisbet, E.G., Baker, A., Kelly, B.F.J., 2015. Assessing connectivity between an overlying aquifer and a coal seam gas resource using methane isotopes, dissolved organic carbon and tritium. Sci. Report. 5, 15996.

Jones, J., Mulholland, P., 1998a. Influence of drainage basin topography and elevation on carbon dioxide and methane supersaturation of stream water. Biogeochemistry 40 (1), 57–72.

Jones, J.B., Mulholland, P.J., 1998b. Methane input and evasion in a hardwood forest stream: effects of subsurface flow from shallow and deep pathways. Limnol. Oceanogr. 43 (6), 1243–1250.

Kanduc, T., Szramek, K., Ogrinc, N., Walter, L.M., 2007. Origin and cycling of riverine inorganic carbon in the Sava River watershed (Slovenia) inferred from major solutes and stable carbon isotopes. Biogeochemistry 86, 137–154.

Keeling, C.D., 1958. The concentration and isotopic abundances of atmospheric carbon dioxide in rural areas. Geochim. Cosmochim. Acta 13, 322–334.

Khadka, M.B., Martin, J.B., Jin, J., 2014. Transport of dissolved carbon and CO_2 degassing from a river system in a mixed silicate and carbonate catchment. J. Hydrol. 513, 391–402.

Kone, Y.J.M., Abril, G., Delille, B., Borges, A.V., 2010. Seasonal variability of methane in the rivers and lagoons of Ivory Coast (West Africa). Biogeochemistry 100 (1–3), 21–37.

Lee, J.-M., Kim, G., 2006. A simple and rapid method for analysing radon in coastal and ground waters using a radon-in-air monitor. J. Environ. Radioact. 89, 219–228.

Li, S., Lu, X.X., He, M., Zhou, Y., Li, L., Ziegler, A.D., 2012. Daily CO_2 partial pressure and CO_2 outgassing in the upper Yangtze River basin: a case study of the Longchuan River, China. J. Hydrol. 466-467, 141–150.

Looman, A., Santos, I.R., Tait, D.R., Webb, J.R., Sullivan, C.A., Maher, D.T., 2016. Carbon cycling and exports over diel and flood-recovery timescales in a subtropical rainforest headwater stream. Sci. Total Environ. 550, 645–657.

Macklin, P.A., Maher, D.T., Santos, I.R., 2014. Estuarine canal estate waters: hotspots of CO2 outgassing driven by enhanced groundwater discharge? Mar. Chem. 167, 82–92.

Maher, D.T., Eyre, B.D., 2011. Insights into estuarine benthic dissolved organic carbon (DOC) dynamics using δ^{13}C-DOC values, phospholipid fatty acids and dissolved organic nutrient fluxes. Geochim. Cosmochim. Acta 75 (7), 1889–1902.

Maher, D., Eyre, B.D., 2012. Carbon budgets for three autotrophic Australian estuaries: implications for global estimates of the coastal air-water CO_2 flux. Glob. Biogeochem. Cycles 26 (GB1032).

Maher, D.T., Santos, I.R., Tait, D.R., 2014. Mapping methane and carbon dioxide concentrations and δ^{13}C values in the atmosphere of two Australian coal seam gas fields. Water Air Soil Pollut. 225 (12), 1–9.

Maher, D.T., Cowley, K., Santos, I.R., Macklin, P.A., Eyre, B.D., 2015. Methane and carbon dioxide dynamics in a subtropical estuary over a diel cycle: insights from automated in situ radioactive and stable isotope measurements. Mar. Chem. 168, 69–79.

Mann, P.J., Spencer, R.G.M., Dinga, B.J., Poulsen, J.R., Hernes, P.J., Fiske, G., Salter, M.E., Wang, Z.A., Hoering, K.A., Six, J., Holmes, R.M., 2014. The biogeochemistry of carbon across a gradient of streams and rivers within the Congo Basin. J. Geophys. Res. Biogeosci. 119, 687–702.

Mehring, A.S., Lowrance, R.R., Helton, A.M., Pringle, C.M., Thompson, A., Bosch, D.D., Vellidis, G., 2013. Interannual drought length governs dissolved organic carbon dynamics in blackwater rivers of the western upper Suwannee River basin. J. Geophys. Res. Biogeosci. 118 (4), 1636–1645.

Middelburg, J., Nieuwenhuize, J., Iversen, N., Høgh, N., de Wilde, H., Helder, W., Seifert, R., Christof, O., 2002. Methane distribution in European tidal estuaries. Biogeochemistry 59 (1–2), 95–119.

Moyer, R.P., Powell, C.E., Gordon, D.J., Long, J.S., Bliss, C.M., 2015. Abundance, distribution, and fluxes of dissolved organic carbon (DOC) in four small sub-tropical rivers of the Tampa Bay Estuary (Florida, USA). Appl. Geochem. 63, 550–562.

Mulholland, P.J., 2003. Large scale patterns in dissolved organic carbon concentration, flux, and sources. In: Findlay, S.E.G., Sinsabaugh, R.L. (Eds.), Aquatic Ecosystems: Interactivity of Dissolved Organic Matter. Academic Press, San Diego, CA, pp. 139–159.

Office of Water, N.S.W, 2015. Real Time Data - Richmond River Basin. NSW Department of Primary Industries. Retrieved from http://realtimedata.water.nsw.gov.au/water.stm.

Onstad, G.D., Canfield, D.E., Quay, P.D., Hedges, J.I., 2000. Sources of particulate organic matter in rivers from the continental USA: lignin phenols and stable carbon isotope compositions. Geochim. Cosmochim. Acta 64, 3359–3546.

Palmer, S.M., Hope, D., Billett, M.F., Dawson, J.J.C., Bryant, C.L., 2001. Sources of organic and inorganic carbon in a headwater stream: evidence from carbon isotope studies. Biogeochemistry 52, 321–338.

Pawellek, F., Veizer, J., 1994. Carbon cycle in the upper Danube and its tributaries: $\delta^{13}C_{DIC}$ constraints. Isr. J. Earth Sci. 43, 187–194.

Pelletier, G., Lewis, E., Wallace, D., 2007. Olympia: CO_2SYS. Xls: A Calculator for the CO_2 System in Seawater for Microsoft Excel/VBA. Washington State Department of Ecology/Brookhaven National Laboratory.

Perkins, A.K., Santos, I.R., Sadat-Noori, M., Gatland, J.R., Maher, D.T., 2015. Groundwater seepage as a driver of CO_2 evasion in a coastal lake (Lake Ainsworth, NSW, Australia). Environ. Earth Sci. 74, 779–792.

Peterson, R.N., Santos, I.R., Burnett, W.C., 2010. Evaluating groundwater discharge to tidal rivers based on a Rn-222 time-series approach. Estuar. Coast. Shelf Sci. 86 (2), 165–178.

Ran, L., Lu, X.X., Sun, H., Han, J., Li, R., Zhang, J., 2013. Spatial and seasonal variability of organic carbon transport in the Yellow River, China. J. Hydrol. 498, 76–88.

Raymond, P.A., Cole, J.J., 2001. Gas exchange in rivers and estuaries: choosing a gas transfer velocity. Estuaries 24, 312–317.

Raymond, P.A., Zappa, C.J., Butman, D., Bott, T.L., Potter, J., Mulholland, P., Laursen, A.E., McDowell, W.H., Newbold, D., 2012. Scaling the gas transfer velocity and hydraulic geometry in streams and small rivers. Limnol. Oceanogr. Fluids Environ. 2, 41–53.

Richey, J.E., Melack, J.M., Aufdenkampe, A.K., Ballester, V.M., Hess, L.L., 2002. Outgassing from Amazonian rivers and wetlands as a large tropical source of atmospheric CO_2. Nature 416 (6881), 617–620.

Ruiz-Halpern, S., Maher, D.T., Santos, I.R., Eyre, B.D., 2015. High CO_2 evasion during floods in an Australian subtropical estuary downstream from a modified acidic floodplain wetland. Limnol. Oceanogr. 60 (1), 42–56.

Rulík, M., Čáp, L., Hlaváčová, E., 2000. Methane in hyporheic zone of a small lowland stream (Sitka, Czech Republic). Limnologica 30 (4), 359–366.

Sadat-Noori, M., Maher, D.T., Santos, I.R., 2015. Groundwater discharge as a source of dissolved carbon and greenhouse gases in a subtropical estuary. Estuar. Coasts 39, 639–656.

Santos, I.R., Niencheski, F., Burnett, W., Peterson, R., Chanton, J., Andrade, C.F.F., Milani, I.B., Schmidt, A., Knoeller, K., 2008. Tracing anthropogenically-driven groundwater discharge into a coastal lagoon from southern Brazil. J. Hydrol. 353 (3–4), 275–293.

Santos, I.R., Dimova, N., Peterson, R., Mwashote, B., Chanton, J., Burnett, W.C., 2009. Extended time series measurements of submarine groundwater discharge tracers (^{222}Rn and CH_4) at a coastal site in Florida. Mar. Chem. 113 (1–2), 137–147.

Santos, I.R., Beck, M., Brumsack, H.-J., Maher, D.T., Dittmar, T., Waska, H., Schnetger, B., 2015. Porewater exchange as a driver of carbon dynamics across a terrestrial-marine transect: insights from coupled ^{222}Rn and pCO_2 observations in the German Wadden Sea. Mar. Chem. 171, 10–20.

Schubert, C.J., Lucas, F.S., Durisch-Kaiser, E., Stierli, R., Diem, T., Scheidegger, O., Vazquez, F., Muller, B., 2010. Oxidation and emission of methane in a monomictic lake (Rotsee, Switzerland). Aquat. Sci. 72, 455–466.

Schulte, P., van Geldern, R., Freitag, H., Karim, A., Négrel, P., Petelet-Giraud, E., Probst, A., Probst, J.-L., Telmer, K., Veizer, J., Barth, J.A.C., 2011. Applications of stable water and carbon isotopes in watershed research: weathering, carbon cycling, and water balances. Earth Sci. Rev. 109, 20–31.

Shin, W.J., Chung, G.S., Lee, D., Lee, K.S., 2011. Dissolved inorganic carbon export from carbonate and silicate catchments estimated from carbonate chemistry and $\delta^{13}C_{DIC}$. Hydrol. Earth Syst. Sci. 15, 2551–2560.

Sholkovitz, E.R., 1976. Flocculation of dissolved organic and inorganic matter during the mixing of river water and seawater. Geochim. Cosmochim. Acta 40, 831–845.

Smith, B.N., Epstein, S., 1971. Two categories of $^{13}C/^{12}C$ ratios for higher plants. Plant Physiol. 47 (3), 380–384.

Stanley, E.H., Casson, N.J., Christel, S.T., Crawford, J.T., Loken, L.C., Oliver, S.K., 2015. The ecology of methane in streams and rivers: patterns, controls, and global significance. Ecol. Appl.

Striegl, R.G., Dornblaser, M.M., Aiken, G.R., Wickland, K.P., Raymond, P.A., 2007. Carbon export and cycling by the Yukon, Tanana, and porcupine rivers, Alaska, 2001–2005. Water Resour. Res. 43 (W02411).

Striegl, R.G., Dornblaser, M.M., McDonald, C.P., Rover, J.R., Stets, E.G., 2012. Carbon dioxide and methane emissions from the Yukon River system. Glob. Biogeochem. Cycles 26 (4), GB0E05.

Tait, D.R., Maher, D.T., Santos, I.R., 2015. Seasonal and diurnal dynamics of atmospheric radon, carbon dioxide, methane, δ^{13}C-CO_2 and δ^{13}C-CH_4 in a proposed Australian coal seam gas field. Water Air Soil Pollut. 226 (10).

Tan, P.L., George, D., Comino, M., 2015. Cumulative risk management, coal seam gas, sustainable water, and agriculture in Australia. Int. J. Water Resour. Dev. 31 (4), 682–700.

Taylor, C.B., Fox, V.J., 1996. An isotopic study of dissolved inorganic carbon in the catchment of the Waimakariri River and deep ground water of the North Canterbury plains, New Zealand. J. Hydrol. 186, 161–190.

Turmel, M.C., Turgeon, J.M.L., Cloutier-Hurteau, B., Courchesne, F., 2005. Seasonal variations of the transport of dissolved organic carbon in the intermittent stream draining the Hermine headwater catchment on the Canadian Shield. Rev. Sci. Eau 18 (3), 353–380.

Wallin, M.B., Löfgren, S., Erlandsson, M., Bishop, K., 2014. Representative regional sampling of carbon dioxide and methane concentrations in hemiboreal headwater streams reveal underestimates in less systematic approaches. Glob. Biogeochem. Cycles 28 (4), 465–479.

Wang, F.S., Wang, Y., Zhang, J., Xu, H., Wei, X., 2007. Human impact on the historical change of CO_2 degassing flux in river Changjiang. Geochem. Trans. 8.

Weiss, R.F., 1974. Carbon dioxide in water and seawater: the solubility of a non-ideal gas. Mar. Chem. 2, 203–215.

Westhorpe, D.P., Mitrovic, S.M., 2012. Dissolved organic carbon mobilisation in relation to variable discharges and environmental flows in a highly regulated lowland river. Mar. Freshw. Res. 63, 1218–1230.

Whalen, S.C., 2005. Biogeochemistry of methane exchange between natural wetlands and the atmosphere. Environ. Eng. Sci. 22 (1), 73–94.

Whiticar, M.J., Faber, E., 1986. Methane oxidation in sediment and water column environments - isotope evidence. Org. Geochem. 10 (4–6), 759–768.

Whiticar, M.J., Faber, E., Schoell, M., 1986. Biogenic methane formation in marine and freshwater environments: CO_2 reduction vs. acetate fermentation - isotope evidence. Geochim. Cosmochim. Acta 50 (5), 693–709.

Wilcock, R.J., Sorrell, B.K., 2008. Emissions of greenhouse gases CH4 and N2O from low-gradient streams in agriculturally developed catchments. Water Air Soil Pollut. 188 (1–4), 155–170.

Yamamoto, S., Alcauskas, J.B., Crozier, T.E., 1976. Solubility of methane in distilled water and seawater. J. Chem. Eng. Data 21 (1), 78–80.

Yang, C., Telmer, K., Veizer, J., 1996. Chemical dynamics of the 'St. Lawrence' riverine system: δD_{H2O}, $\delta^{18}O_{H2O}$, $\delta^{13}C_{DIC}$, $\delta^{34}S_{sulfate}$, and dissolved $^{87}Sr/^{86}Sr$. Geochim. Cosmochim. Acta 60, 851–866.

Yao, G., Gao, Q., Wang, Z., Huang, X., He, T., Zhang, Y., Jiao, S., Ding, J., 2007. Dynamics of CO_2 partial pressure and CO_2 outgassing in the lower reaches of the Xijiang River, a subtropical monsoon river in China. Sci. Total Environ. 376 (1–3), 255–266.